β1 integrin dependent Rac/group I PAK signaling mediates YAP activation of Yes associated protein 1 (YAP1) via NF2/merlin.

Hiba Sabra, Molly Brunner, Vinay Mandati, Bernhard Wehrle-Haller, Dominique Lallemand, Anne-Sophie Ribba, Genevieve Chevalier, Philippe Guardiola, Marc R. Block, Daniel Bouvard

β1 integrin dependent Rac/group I PAK signaling mediates YAP activation of Yes associated protein 1 (YAP1) via NF2/merlin.

Hiba Sabra[1,2,3], Molly Brunner[1,2,3], Vinay Mandati[4], Bernhard Wehrle-Haller[5], Dominique Lallemand[6], Anne-Sophie Ribba[1,2,3], Genevieve Chevalier[1,2,3], Philippe Guardiola[7], Marc R. Block[1,2,3] and Daniel Bouvard[1,2,3#].

1: INSERM U1209, Institute for Advanced Bioscience, Grenoble, France; 2: CNRS 5309, Institute for Advanced Bioscience, Grenoble, France; 3: Univ. Grenoble Alpes, Institute for Advanced Bioscience, Grenoble, France; 4:Department of Cancer Biology, The Scripps Research Institute, Jupiter, Florida, USA; 5: Dept. of Cell Physiology and Metabolism, Centre Médical Universitaire, University of Geneva, Geneva, Switzerland; CNRS 7654, 6: Ecole Polytechnique, Dept of Biochemistry, Palaiseau, France; 7: Centre Hospitalier Universitaire and University of Angers, SNP Plateform, Institute for Biological Health, Transcriptome and Epigenomic, Angers, France.

Running title: *Cell adhesion control of YAP activation*

To whom correspondence should be addressed: Dr. Daniel Bouvard, Institute for Advanced Bioscience, Univ. Grenoble Alpes, Site Santé, BP170 La Tronche 38042 Grenoble cedex 9 France. Telephone: +33 476549551; Fax: +33 476549425. Email: daniel.bouvard@univ-grenoble-alpes.fr

Key words: Integrin, Rac, Adhesion, Merlin, YAP

Abstract

Cell adhesion to the extracellular matrix or to surrounding cells plays a key role in cell proliferation and differentiation, and is critical for proper tissue homeostasis. An important pathway in adhesion-dependent cell proliferation is the Hippo signaling cascade, which is coregulated by the transcription factors Yes-associated protein 1 (YAP1) and transcriptional coactivator with PDZ-binding motif (TAZ). However, how cells integrate extracellular information at the molecular level to regulate YAP1's nuclear localization is still puzzling. Herein, we investigated the role of β1 integrins in regulating this process. We found that β1 integrin–dependent cell adhesion is critical for supporting cell proliferation in mesenchymal cells both in vivo and in vitro. β1 integrin–dependent cell adhesion relied on the relocation of YAP1 to the nucleus after the downregulation of its phosphorylated state mediated by large tumor suppressor gene 1 and 2 (LATS1/2). We also found that this phenotype relies on β1 integrin–dependent local activation of the small GTPase Rac1 at the plasma membrane to control the activity of P21 (RAC1)-activated kinase (PAK) of group 1. We further report that the regulatory protein merlin (neurofibromin 2, NF2) interacts with both YAP1 and LATS1/2 via its C-terminal moiety and FERM domain, respectively. PAK-mediated merlin phosphorylation on Ser-518 reduced merlin's interactions with both LATS1/2 and YAP1, resulting in YAP1 dephosphorylation and nuclear shuttling. Our results highlight Rac1/PAK1 as major players in YAP1 regulation triggered by cell adhesion.

INTRODUCTION

Cell adhesion to the extracellular matrix or to surrounding cells plays a key role in cell proliferation, differentiation or apoptosis, and consequently is critical for proper development or tissue homeostasis (1). On the other hand, deregulation of this process often contributes to pathological disorders such as tumor formation, growth and metastasis (2), exemplified by one of

the hallmarks of cell transformation: the anchorage-independent growth (3,4).

Hippo signaling was identified as an important regulatory pathway that restricts cell proliferation, thereby controlling organ size and morphogenesis (5,6). This is achieved mainly through the control of two transcriptional co-activators: Yes-associated protein (YAP1) and transcriptional coactivator with PDZ-binding motif (TAZ/WWTR1). Upon restrictive proliferative conditions, these molecules are phosphorylated by the products of the large tumor suppressor gene 1 and 2 (LATS1/2), thereby creating a binding site for 14-3-3 proteins which binding prevents their nuclear import. As a consequence, phosphorylated forms of YAP/TAZ are sequestered in the cytoplasm (7,8).

While originally described as the main switch to block cell proliferation when confluency is reached, it has become clear that the hippo signaling pathway is integrating several inputs such as cell density, cell geometry, matrix stiffness, metabolic status and serum composition (9). Indeed, activation of YAP/TAZ mediated transcriptions, which correlates with their nuclear localization, is tightly controlled by cell matrix adhesion (10,11). This process explains why cells are dependent on matrix adhesion for a full mitogenic response to growth factors exposure (12). Loss of cell adhesion to the ECM is known to induce an increase in cyclic AMP (cAMP) which is correlated with the inhibition of mitogenic signaling (13). Since YAP/TAZ activities are also inhibited by cAMP, this raise in cAMP was proposed as the main factor to regulate YAP/TAZ upon cell detachment, potentially mediated though downstream players such as RhoA or LATS1/2 (10,14). On the other hand, cell adhesion to cell matrix proteins was shown to trigger YAP nuclear localization through an integrin/FAK/Src axis (15). Despite these findings, the molecular mechanism downstream of FAK/Src to control subcellular YAP/TAZ localization remains ill-defined and has never been directly investigated.

Initially, RhoA was identified as a critical regulator of YAP, however more recently Rac1 and Cdc42 were also found to be involved in its regulation (16-18). So far, how small RhoA family GTPases regulate YAP nuclear translocation remains elusive. Knowing that integrins are key regulators of this GTPase class, we wondered whether β1 integrins might regulate YAP by controlling RhoA GTPases.

Herein, we address the mechanistic role of β1 integrins in the regulation of YAP localization and thereby cell proliferation. We found that β1 integrin-dependent cell adhesion was critical for supporting cell proliferation in mesenchymal cells both *in vivo* and *in vitro* by controlling YAP signaling rather than MAPK cascade. Mechanistically, we showed that β1 integrins are required for localizing the GTPase Rac1 at plasma membrane extensions. There, Rac1 activates its effector PAK1 and initiates in a merlin dependent manner the nuclear translocation of YAP. Indeed, we found that merlin binds LATS via its FERM N-terminal domain but also interacts with YAP with its C-terminal moiety. The interactions between merlin and YAP or LATS are down regulated upon phosphorylation by PAK1 at S518. Altogether our data revealed a novel signaling pathway orchestrated by β1 integrins to locally activate a Rac1/PAK1 cascade and negatively regulate the inhibitory protein merlin.

RESULTS

β1 integrins regulate mesenchymal cell proliferation in a MAPK independent manner.

To explore the function of β1 integrins in bone tissue, we inactivated the β1 integrin gene in osteoblasts using Osterix-driven Cre recombinase expression. Mice with an osteoblast specific β1-integrin deletion survived to adulthood but suffered from a growth deficit along with a significant decrease in the absolute number of osteoblasts (Fig. 1A). Since β1 integrins are known to regulate cell proliferation we wondered whether the reduced osteoblast numbers observed could be due to a reduced proliferative capability of those cells. While TUNEL staining did not reveal any significant difference in apoptotic cell number (Fig. 1B,

1C), a significant reduction in BrdU incorporation was observed in mutant animals (Fig. 1D, 1E). Similarly, *in vitro*, the loss of β1 integrins in isolated osteoblasts, resulted in a significant proliferation defect (Fig. 1F). To rule out any osteoblast specific phenotype we isolated mouse embryonic fibroblasts (MEFs) and confirmed that the loss of β1 integrin expression was associated with a reduced proliferative capability of the cells (Fig. 1G). Although it was proposed that integrins are important regulators of ERK signaling (19), we could not rescue the proliferation defect of β1 integrin deficient cells by activating the MAPK/ERK pathway (Fig. 1H). In addition, we did not detect any significant modification of ERK phosphorylation when β1 integrin deficient cells were compared to wild-type cells (not shown).

β1 integrins are required for YAP nuclear localization and cell proliferation.

YAP dependent gene expression has emerged as an important pathway regulating cell proliferation (20). Moreover, it was recently reported that YAP nuclear localization is controlled in a cell adhesion manner through integrins and Src/FAK (21), therefore we first asked whether the loss of β1 integrin expression was indeed associated with a defect in YAP nuclear localization and that might account for the reduced proliferation observed in β1 deficient cells.

When compared to wild-type cells that displayed a prominent YAP/TAZ nuclear localization, the lack of β1 integrins was correlated with a strong relocation of these proteins within the cytoplasm (Fig. 2A, 2B). This observation was confirmed with other clones analyzed (Fig. 2C), as well as in cell lines stably expressing a flag tagged YAP (Fig. 2D). To further evaluate the involvement of ERK/MAPK pathway in controlling YAP nuclear localization downstream of β1 integrins, we isolated MEF cells from mouse bearing a constitutively active allele of K-Ras (K-Ras^{G12D}) (22) with one or two deleted alleles of the β1 integrin gene. Even in the presence of the activated allele of K-Ras, YAP was mainly cytoplasmic as soon as the β1 integrin chain was genetically ablated (Fig. 2E). Notably, YAP/TAZ nuclear localization was completely restored upon re-expression of the human β1 integrin subunit in β1 deficient mouse cells, showing a direct relationship between β1 expression and the nuclear localization of YAP/TAZ (Fig. 2A, 2B). In line with these observations, biochemical fractionations revealed a decrease in the nuclear pool of YAP in β1 deficient cells (Fig. 2F). Along with the reduced level of nuclear YAP, the expression of its target genes was also downregulated in β1 deficient cells (Fig. 3A). YAP was shown to be sequestered in the cytoplasm by 14-3-3 proteins after the activation of its upstream protein kinase LATS (7). In good agreement with this, we noticed that the phosphorylation of YAP on S127 (required for 14-3-3 binding) increased upon the deletion of β1 integrins as well as the ratio of activated (phosphorylated) versus total form of LATS (Fig. 3B). Therefore, taking together, these data confirmed that β1 integrins are important players in controlling YAP nuclear localization likely in a LATS dependent manner.

Having shown that β1 integrins regulate nuclear localization of YAP, we wondered whether the proliferation defect that we observed upon removal of β1 integrins was the consequence of YAP nuclear translocation. Our data highlighted that LATS dependent phosphorylation of YAP was upregulated in β1 deficient cells. Therefore, we stably expressed in those cells a non phosphorylable form of YAP. The expression of YAP^{5SA} in β1 integrin null cells, relocated YAP into the nucleus and up-regulated its target genes (Fig. 3C, 3D). Importantly, the expression of YAP^{5SA} fully restored β1$^{-/-}$ cell proliferation capabilities as quantified by BrdU incorporation (Fig. 3E). Therefore, our data highlighted the important role of YAP signaling in the control of cell proliferation downstream of β1 integrins.

Finally, to confirm this view, we performed unbiased transcriptomic analyses on wild-type and β1 integrin deficient cells under optimal growth conditions. With the defined filtering and statistical criterion, 800 probes representing 555 well annotated genes were identified as being differentially expressed between the 2 considered groups (Figure S1). Known YAP/TEAD target genes were significantly

down-regulated in $\beta1^{-/-}$ cells. Among those were ANKRD1, CTGF, and CYR61 (Fig. S2). These results confirmed our previous RT-qPCR analyses (Fig. 3A, 3D). Consistent with the above mentioned proliferation defect, a number of cell cycle regulators were also deregulated (Fig. S1). To directly estimate whether the YAP/TEAD complex might impact the expression of those important cell cycle regulators we analyzed $p19^{Arf}$, $p21^{CIP}$ and cyclin D2 expression by RT-qPCR in cell expressing YAP^{5SA}. In contrast to what was measured in β1 deficient cells, the expression of YAP^{5SA} in wild-type cells was able to upregulated cyclin D2 and downregulated $p19^{Arf}$ but not $p21^{CIP}$ when compared to control cells (Fig. 3E). This strongly suggests that some important cell cycle regulators are transcriptionally modified by the YAP/TEAD complex.

Rac1, but neither Cdc42 nor RhoA, controls YAP nuclear localization downstream of β1 integrins

While accumulating evidences pinpointed a role of FAK and Src in integrin dependent control of the hippo pathway (21), little is known on downstream effectors. On the other hand, members of the Rho GTPase family were shown to be involved in the control of YAP activity (10,23,24). It is well known that integrins also play a critical role in the activation or the coupling of Rho GTPases with their effectors. Therefore, we wondered whether YAP nuclear localization driven by β1 integrins might also be regulated by Rho GTPases and if so, which one.

To address this question, we used β1 deficient osteoblasts that displayed a dramatic defect in YAP nuclear localization to generate stable cell lines expressed constitutively activated forms of RhoA, Rac1, and Cdc42. Then, we analyzed which Rho GTPase was able to induce the relocation of YAP within the nucleus. Surprisingly, activated RhoA was unable to restore the nuclear localization of YAP (Fig. 4A, 4B). In line with this observation, we neither observed any significant difference in RhoA-GTP levels in wild type versus β1 deficient cells, nor any change in its cellular distribution (Fig. 4C, 4D). In sharp contrast, $Rac1^{G12V}$ expression (and to a lower extend $Cdc42^{G12V}$) was associated with a significant increase in YAP nuclear localization in $\beta1^{-/-}$ cells (Fig. 4A, 4E). Importantly, $Rac1^{G12V}$ expression restored YAP nuclear localization in β1 deficient cells but not their spreading defect (Fig. 4F). This strongly suggested that Rac1 and Cdc42 might act downstream of β1 integrins in the signaling pathway that regulates YAP nuclear localization.

Since the expression of constitutively activated Cdc42 and Rac1 could activate common effectors such as PAK, we wondered whether both small GTPase proteins were physiologically involved in this regulation. Hence, to discriminate between Rac1 and Cdc42, we specifically inhibited their activities and analyzed YAP subcellular localization. The expression of a dominant negative form of Cdc42 ($Cdc42^{N17}$) did not result in any significant YAP redistribution in wild type cells (Fig. 5A and S3). In sharp contrast, the inhibition of Rac1 activity either pharmacologically with ETH1864 or by the expression of a dominant negative form ($Rac1^{N17}$) led to a significant YAP redistribution to the cytoplasm (Fig. 5A and S3).

As our previous data, pointed out for a major role of Rac1, we next analyzed whether the expression of constitutively active Rac1 could reverse the proliferation defect observed in β1 deficient cells. Indeed, $Rac1^{G12V}$ expression in β1 deficient cells restored proliferation up to the level of control cells (Fig. 5B). This suggested that both Rac1 and YAP were in a common pathway to regulate β1 dependent cell proliferation. Indeed, the expression of $Rac1^{G12V}$ in β1 deficient cells induced a decrease in YAP phosphorylation to a comparable level to the one observed in $\beta1^{f/f}$ cells (Fig. 5C). From these results, we concluded that Rac1 is involved in YAP signaling upon β1 dependent cell adhesion. Surprisingly, quantification of $Rac1^{GTP}$ levels in $\beta1^{f/f}$ and $\beta1^{-/-}$ in whole cell lysates did not reveal any significant difference (Fig 5D). This discrepancy suggested that an altered Rac1 localization, rather than a global defect in its activity per se, resulted in YAP mislocalization observed in β1 deficient cells. Supporting this hypothesis, it was reported that cell adhesion regulates Rac1 plasma membrane localization (25), although the role of β1 integrin in this

process was not addressed. To address this question directly, we performed immunostaining to analyze endogenous Rac1 localization in $\beta1^{f/f}$ and $\beta1^{-/-}$ cells. As expected, in wild-type cells, Rac1 frequently accumulated at protrusive cell edges; however, this localization was strongly reduced upon β1 removal (Fig. 5E, 5F). In order to orchestrate actin dynamics, it was previously shown that Rac1 recruits cortactin at cell lamellipodia (26). Further supporting the defect in Rac1 membrane localization in β1 deficient cells, we observed that cortactin localization at cell edges was also significantly reduced in mutant cells (Fig. 5G, 5H).

PAK1, a merlin inhibitor, acts downstream of Rac1

On the search of how Rac1 could affect YAP nuclear localization, we focused our attention on its effectors, the PAK family. Indeed, PAK1/2 are activated at the plasma membrane by Rac1 and/or Cdc42, where they regulate membrane dynamics (27,28). First, we asked whether impaired Rac1 targeting to the plasma membrane was translated into a defect in PAK1 activity. As expected, this activity, monitored by its phosphorylation, was reduced in β1 deficient cells but restored upon the re-expression of β1 integrins (Fig. 6A). Consistent with the defect in Rac1 recruitment to the plasma membrane, PAK membrane localization was reduced in β1 deficient cells but restored upon the expression of the constitutively active $Rac1^{G12V}$ (Fig 6B). Altogether these results supported the view that β1 integrins by regulating Rac1 localization at the plasma membrane would promote the recruitment and activation of its downstream effectors such as PAK and cortactin.

Having shown that Rac1 was required for controlling YAP nuclear translocation downstream of β1 integrins, and that PAK1 activity was reduced in β1 deficient cells, we wondered whether YAP nuclear translocation was also dependent on PAK activity. We transiently expressed in both wild-type and β1 deficient cells the constitutively active mutant of PAK1 ($PAK1^{T423E}$) and analyzed YAP subcellular localization. As previously observed with the expression of activated Rac1, the expression of constitutively active PAK1 also rescued the defective YAP nuclear localization in β1 deficient cells (Fig 6C); while the pharmacological inhibition of group I PAK using IPA3 (a specific inhibitor of this class) in wild-type cells, significantly reduced it (Fig. 6D). Similarly, the expression of a dominant negative form of PAK1 ($PAK1^{K299R}$) resulted in the delocalization of YAP out of the nucleus (Fig. 6E). Altogether, our data strongly suggest that β1 integrins control YAP nuclear localization in a Rac1/PAK1 dependent manner.

Src acts downstream of β1 integrin but upstream of Rac1/PAK1.

As mentioned before, Src was described to mediate YAP nuclear translocation downstream of integrins. Src was also shown to be required for Rac1 activity (29,30). Therefore, we wondered whether the loss of β1 integrin expression also impaired Src activity. Indeed, we observed that in $\beta1^{-/-}$ cells Src was not properly activated (Fig. 7A). Consistent with this observation, the expression of a constitutively activated Src rescued β1 deficient cell proliferation as well as YAP nuclear accumulation (Fig. 7B, 7C, 7D) and PAK1 activation (Fig. 7E). Yet, the inhibition of Rac1 was still able to block YAP nuclear translocation (Fig. 7D). Altogether, these data clearly indicated that Src is downstream of β1 integrins and upstream of Rac1 in this signaling pathway.

β1 integrins control YAP nuclear translocation through merlin.

Next, we hypothesized that merlin, a known regulator of LATS1/2 (31), might be regulated by PAK1 and this might be an important step in how β1 integrin mediated YAP nuclear translocation. Indeed, together with PKA, PAK was described to induce merlin inhibition by phosphorylation of the S518 residue. Monitoring merlin phosphorylation by Western blotting revealed a decrease in S518 phosphorylation in β1 deficient cells when compared to parental $\beta1^{f/f}$ cells (Fig. 8A). Such modification should favor the recruitment and activation of LATS.

Indeed, merlin phosphorylation at S518 was proposed to stimulate the intramolecular FERM to C-terminal interaction (32). In its non-phosphorylated form merlin adopts an open conformation in which the FERM domain interacts with LATS while the C-terminal interacts with Amot (another important effector of YAP signaling).

To confirm this, we preformed GFP-trap experiments with several merlin domains bearing or not mutations. As reported by others, LATS was shown to interact with the FERM domain of merlin but not with its C-terminal moiety. Moreover, this interaction was significantly reduced with the phospho-mimetic S158D mutant (Fig 8B). The deletion of a stretch of 7 amino-acids within the FERM domain (named blue-box) was reported to act as a dominant negative form when expressed both in Drosophila as well as in Mammals. Of importance, LATS interaction with merlin was strongly reduced in the blue-box mutant as compared to the full-length or FERM domain of merlin (Fig. 8B). We took advantage of this mutant (that inhere we named $NF2^{BB}$), and generated stable cell lines expressing either a wild type or a blue box mutated form of merlin. Expression the $NF2^{BB}$ mutant in β1 deficient cells, restored YAP nuclear localization (Fig 8C,8D) suggesting that i) merlin was required for YAP nuclear translocation downstream of β1 integrins and ii) the recruitment of LATS by merlin was important in this regulation. Consistent with these results, expressing $NF2^{BB}$ mutant in β1 deficient cells also reduced YAP phosphorylation (Fig. 8E), restored cell proliferation (Fig. 8F), and YAP target genes (Fig. 8G). Altogether, our data strongly supported the view that during cell spreading, β1 integrins mediated the activation of the Rac1/PAK1 axis to phosphorylate and inactivate merlin resulting in fine in LATS inactivation and YAP dephosphorylation. Finally, if this assumption were correct, the inhibition of PAK1 activity should block YAP nuclear translocation in a merlin and LATS dependent manner. We analyzed YAP subcellular localization in IPA3-treated $\beta1^{f/f}$ cells expressing or not the $NF2^{BB}$ mutant. As expected, the inhibition of PAK1 significantly reduced YAP nuclear localization in control cells while it had no significant effect in $NF2^{BB}$ expressing cells, indicating that PAK1 was involved in YAP nuclear translocation upstream of merlin (Fig. 8H). An identical result was also observed when a specific Rac inhibitor was used (Fig. 8H).

Merlin acts as a scaffold to bring LATS and YAP in close vicinity.

Together with others, our data favor the view that the assembly of a merlin centered inhibitory complex including LATS and YAP within the cells inhibits YAP activity. The presence of such a complex at plasma membrane extensions was supported by immunofluorescence staining of the cells. Indeed, we observed a clear colocalization between YAP and LATS in the one hand, and YAP and merlin/NF2 in the other (Fig. 9A). Next, the staining of YAP and pYAP indicated that this membrane pool of YAP was phosphorylated, Indeed the staining of phosphorylated YAP was much stronger in β1 integrin deficient cells, in line with the view that plasma membrane extensions were important sites of YAP phosphorylation (Fig. 9B).

It is noteworthy that in wild-type cells, Rac1 colocalized together with YAP at the cell edges while this colocalization was strongly reduced upon β1 integrins removal (Fig. 9C), We wondered whether proteins recruited at cell edges in a Rac1 dependent manner could also colocalize with YAP. Cells stably expressing RFP-cortactin showed an extensive colocalization during cell spreading, showing that YAP is enriched in protrusive membrane region and suggested a proximity between a Rac1 based signaling with YAP (Fig. 9D).

To further characterize such complex, we mapped the interactions between merlin and the different partners involved in YAP regulation. As mentioned above, LATS interaction with merlin was previously reported on the N-terminal FERM domain while the Amot was mapped to the C-terminal part of merlin (33). Since YAP could interact with both LATS and Amot, we wondered which part of merlin was required for its putative interaction with YAP. We used HEK293 cells to expressed either the full length GFP-merlin, the GFP-merlin FERM

domain, or GFP-merlin C-terminal moiety. YAP and LATS association with merlin were analyzed after GFP pulldown. In contrast to LATS that interacts with merlin via its FERM domain, YAP was co-immunoprecipitated with the C-terminal moiety of merlin or full-length merlin but not by the N-terminal FERM domain (Fig. 10A). Altogether, these results strongly suggested that merlin serves as a scaffolding protein to bring in close contact the protein kinase LATS with its substrate YAP. Indeed, the phosphorylation of merlin at S518 favors the close conformation of merlin, and reduced its interaction with YAP compared to wild-type merlin (Fig. 10A). Since the loss of β1 integrin was associated with a reduced merlin phosphorylation at S518, this could be translated into a differential interaction between YAP and merlin. Indeed, immuno-precipitating YAP in β1 deficient cells recovered a significant greater amount of merlin from the membrane pool when compare to wild type cells (Fig. 10B). Again, inhibition of PAK1 led to a similar observation (Fig. 10C), strongly suggesting that PAK1 activation downstream of β1 integrins was involved in the control of an inhibitory complex encompassing LATS, merlin and YAP according to the model presented Figure 10D.

DISCUSSION

β1-integrins control cell proliferation in a Rac1/PAK/YAP dependent manner.

Although, pioneering works have shown that integrins orchestrate the recruitment of growth factors and clustering of their receptors at the plasma membrane, (likely via cytoplasmic effectors such as FAK and Src), a clear picture of how integrins are involved in the control of cell proliferation is still missing (34). Recently, integrins and cell-matrix adhesion were proposed to participate in the regulation of the Hippo signaling pathway via Src and Fak (21). However, form these data it was not established what are the downstream effectors of integrin/FAK/Src and how this could be molecularly translated into YAP activation. Herein, we provide a molecular basis of the integrin control YAP nuclear translocation. and decipher the final stage of this regulation.

The loss of β1 integrins was associated with a defect in osteoblast proliferation both in vivo and in vitro. Our work also confirmed β1 integrins as the main cell surface receptors by which these cells are capable of linking YAP nuclear translocation in response to cell adhesion. Our observations are in line with previous reports showing that β1 integrins control cell proliferation in other tissues (4). While our main data were obtained with osteoblasts, we observed a similar behavior in MEFs suggesting that the signaling pathway described herein applies to other adherent cell types. Although we focused our work on non-transformed cells, we recently reported that both β1 integrins and YAP are overexpressed in primary bone tumors in which they have been identified as poor prognostic markers (35). Knowing the role of β1 integrins during tumor progression and their capability to sense the extracellular environment, we can envision that β1 dependent YAP nuclear translocation may play an important role in the tumorigenesis of solid tumors.

While the loss of β1 integrins in osteoblasts was clearly associated with a strong defect in YAP signaling that was responsible for the reduced proliferation observed in mutant cells, an important question that remains to be solved is why β1 integrins are so critically involved in controlling YAP nuclear localization. Indeed, we and others (11) have highlighted a specific role of β1 integrins in YAP nuclear localization. This question is even more intriguing knowing that both β1 and β3 integrins can regulate Fak and Src (36). Clearly additional work focusing on these early signaling events will be required to address this question.

Actin cytoskeleton was proposed to be critical for controlling YAP nuclear translocation but the identification of a clear mechanism was elusive. Actin cytoskeleton remodeling may modulate YAP activity through Rho GTPases family (23,24). Our present data support a critical role for Rac1 rather than RhoA or Cdc42 in good agreement with recent reports showing that Arl4c triggers YAP nuclear translocation via the upregulation of Rac1 while blocking RhoA activity (37). While our data do not highlight any role for RhoA in YAP nuclear translocation

downstream of β1 dependent cell adhesion, we cannot rule out that this small GTPase as an important regulator of actin networks, in turn may control membrane targeting of important players of the hippo pathway under specific conditions. It is noteworthy that during cell spreading, integrin engagement inhibits RhoA activity in order to dynamically regulate actin cytoskeleton re-organization (38). This decrease in RhoA activity timely corresponds to YAP nuclear translocation, therefore a direct role of the latter GTPase in adhesion dependent YAP nuclear translocation is very unlikely. Similarly, suspended cells display an elevated level of RhoA and yet YAP is sequestered in the cytoplasm.

In the future, it will be important to gain a better insight into how those GTPases crosstalk in space and time regarding their activation and recruitment of their downstream effectors and thereby specific outcomes such as actin remodeling or YAP nuclear localization.

Here, we propose an integrated view of how β1 integrins regulate YAP nuclear translocation (Fig. 10D). Indeed, using the expression of an activated form of Rac1 and PAK1 or a mutant of merlin (loss of function), we rescued the defective YAP localization that characterizes β1 deficient cells. On the other hand, blocking Rac1 and PAK activity in control cells impaired YAP nuclear localization. Together these data, with the observation that Rac1 and its effector PAK1 did not accumulate at the plasma membrane in β1 deficient cells strongly support a picture in which β1 integrins regulate Rac1 delivery to locally activate PAK1 that in turn modulates YAP in a merlin dependent manner. Fitting with this view, merlin a well-known PAK substrate is underphosphorylated in β1 deficient cells, a post-translational modification that favors its active state to activate LATS dependent YAP inhibition.

β1 integrins regulate the formation of a YAP inhibitory complex

It appears that several key players such as NF2/merlin and LATS that negatively regulate YAP are also concentrated in plasma membrane extensions. This observation fits with previous data showing that LATS is recruited and activated by NF2/merlin at the cell membrane (31) and with the localization of NF2/merlin in membrane ruffles (39). Our data extended the picture and showed that β1 integrins and PAK1 negatively regulates YAP/merlin interaction at the plasma membrane. The reduced YAP/merlin interaction is likely due to the capacity of PAK1 to phosphorylate merlin at the S518 residue to limit YAP and LATS access. Recently, it has been reported that merlin phosphorylation at S518 reduces its interaction with Amot family members (a YAP interacting partners) (33). On the other hand, Amot recruitment to merlin induces or/and stabilizes merlin open conformation and in turn allows LATS binding on the FERM domain of merlin. Our data would favor such a model, in which merlin YAP and LATS belong to a membrane associated inhibitory complex that may be dissociated upon PAK1 phosphorylation. Indeed, we observed that LATS and YAP interact with non-overlapping domains of merlin. While LATS is recruited on merlin using its FERM domain, YAP interacts with the C-terminal part of merlin. Although our data did not establish whether YAP/merlin interaction is direct or via Amot, they clearly indicate that merlin acts as a scaffold to bring in close proximity LATS with YAP. The β1 dependent regulation of PAK1 increases merlin phosphorylation and thereby decreases YAP and LATS recruitment on merlin. Therefore, we proposed that YAP and LATS are recruited in an inhibitory complex at the plasma membrane orchestrated by merlin. Upon cell adhesion Rac1 and PAK1 are locally activated and induce merlin phosphorylation to disrupt merlin, YAP and LATS complex, a prerequisite for YAP nuclear translocation (Fig. 10D).

While our data provide insights into how YAP is controlled by β1 integrins upon cell adhesion, the mechanism of Rac1 targeting to the plasma membrane by β1 engagement is still elusive albeit extensively described. Recently, FAK, PI3K and Src were shown to regulate YAP nuclear translocation (11), but at the molecular level how those proteins control YAP via LATS was not investigated. It is noteworthy that Rac1 activity is modulated by FAK (40) as well as by

PI3K/Src (41). Our data add to these finding, showing that actually Src belongs to the β1 integrin signaling pathways that controls YAP localization. . Therefore, an open possibility is that FAK and Src dependent regulation of YAP nuclear translocation also relies on a mechanism that converge on the release of YAP from merlin upon Rac1/PAK1 activation.. Our data highlighted that the loss of β1 integrins specifically affects Rac1 at the plasma membrane, thus we could speculate that Src/FAK could be important for Rac1 activation/localization and β1 integrins would specifically regulate Rac1 coupling to its effector PAK. Indeed, similarly to Rac1, Src and FAK were shown to be also activated on endosomes upon growth factor stimulation . Once activated Rac1 is then translocated to the plasma membrane in a microtubule and cell adhesion dependent manner (42). Cell adhesion is then important to regulate microtubule targeting to the plasma membrane (43,44).

EXPERIMENTAL PROCEDURES

Mouse Genetics-Mouse strain with floxed alleles of β1 integrin (*Itgb1*^{tm1Ref}) have been described previously (45) and were kindly provided by Dr R. Fässler (Max Planck Institute, Martinsried, Germany). The *Osx1-GFP:Cre* deletor mouse was described previously (46) and was kindly provided by Dr A. McMahon. Conditional knock-in mice bearing the G12D mutation at the K-Ras locus (*Kras*^{tm4Tyj}) were obtained from the NCI mouse repository and originally generated by Dr T. Jacks (47). Mice were kept under regular conditions of husbandry accordingly to the European rules and approved by the University Ethical committee.

Cell lines and MSC culture-Primary MEFs were isolated at embryonic day 14.5 (E14.5) from K-Ras^{G12D} β1$^{f/f}$ or K-Ras^{G12D} β1$^{+/f}$ embryos using a standard procedure. Cells were immortalized with the large SV40 T antigen. Immortalized K-Ras^{G12D}; β1$^{f/f}$ and K-Ras^{G12D} β1$^{+/f}$ cells were infected with an adenoviral supernatant encoding the Cre recombinase for 1h in PBS supplemented with 2% FCS and 1mM $MgCl_2$. All other cell lines were generated upon retrovirus transduction and transgene expression was verified by Western blotting and immunostaining.

Primary mesenchymal stem cells (MSC) were isolated from wt and β1$^{Ost\text{-}ko}$ bone marrow and selected on their capacity to adhere on plastic (48). The differentiation process was visualized by alkaline phosphatase staining described in (49), and the number of alkaline phosphatase colonies having a diameter higher than 0,5mm was evaluated using a stereomicroscope (Olympus SZX10).

Antibodies and expression vectors-Anti-BrdU, -Flag (M2). Anti-YAP/TAZ, -PhosphoYAP, phosphoLATS, -LATS, -phosphoERK, -ERK, phosphoPAK, were from Cell Signaling (Ozyme, St Quentin en Yvelines France). Mouse β1 integrin (MB1.2) and Rac1 were from BD Biosciences (Le Pont de Claix, France), human β1 integrin 9EG7 was produced from hybridoma. Anti-phospho-ELK, Anti-YAP, αPAK, RhoA were from Santa Cruz (Heidelberg, Germany). NF2 and Actin, were from Sigma Aldrich. β1 integrin clone 4B7R antibody from Abcam (Paris, France) was used. The anti-phosphotyrosine monoclonal antibody 4G10 used as hybridoma supernatant was produced in our laboratory. The human β1-expressing construct was based on the pCL-MFG retroviral vector as described previously (50). pBABEpuro-FlagYAP2 was from Dr. M. Sudol (Addgene #27472). Flag tagged YAP2^{5SA} was from Dr. K.L. Guan (Addgene #27371)) was subcloned into the pQCXIP retroviral vector. pBABEpuro-MEK1^{Q56P} and pBABEpuro$^{ERK2MEK1\text{-}LA}$ were kindly provided by Dr. M. Barbacid. pEGFP-Rac1^{G12V}, pEGFP-Rac1^{N17}, pEGFP-Rac1^{Q61L}, pEGFP-Cdc42^{G12V}, pBABEpuro-EGFP-Cdc42^{N17}, and pEGFP-RhoA^{G14V}were gift from Dr C. Gauthier-Rouvière, pYFP-RhoA was from Dr. A. Mettouchi. The insert GFP-Rac1^{G12V} was subcloned into the retroviral vector pBABEpuro. pCMV6M-PAK1^{T423E}, encoding for PAK1-CA, was from Dr Chernoff (Addgene # 12208). Dominant negative PAK1 was from Dr S. Stromblad.- pBabe-NF2^{wt} and pBabe-NF2^{BB} were from Dr. T. Jacks (Addgene#14116 and #14117, respectively). GST-Rhotekin was from Dr. M. Schwartz (Addgene #15247). IPA3 was

from Sigma Aldrich (l'Isle d'Abeau, France) and ETH1864 from Tocris (RD systems, Lille France)

Transfections and Infections-HEK GP 293 cells (Clontech, St Germain en Laye, France) were transfected with plasmid DNA using ExGen500 Transfection reagent (Euromedex, Souffelweyersheim, France) according to manufacturer's instructions. Osteoblast retroviral infections were performed as previously described (43).

Histomorphometric analysis-Tibiae were fixed and embedded in methyl methacrylate. Sections were deplasticized and stained for Masson-Goldner with hematoxylin (Gill II), acid fuchsin/ponceau xylidine, and phosphomolybdic acid/orange G to stain the cells and osteoid, and light green to stain the mineralized matrix (51). The total absolute number of osteoblasts in the area extending from 150 µm below the growth plate down 2 mm was evaluated and reported.

TUNEL and BrdU in vivo staining assay-Fluorescein "In Situ" Cell Death Detection Kit (Roche, Meylan, France) was used for TUNEL staining. Briefly, bone sections were deparaffinized and hydrated. Antigen retrieval and endogenous peroxidase quenching were performed then TUNEL staining was achieved according to manufacturer's instructions. The TUNEL-positive cells and total cells (DAPI positive) in five areas of periosteum and trabecular bone from each of the mice in the experiments were counted under a 20× objective microscope lens.

For BrdU staining, mice were sacrificed two hours after being injected with BrdU (150µg/g). Following deparaffinization and hydration, sections were treated 20min with HCl 4N, and then antigen retrieval was performed using trypsin 10min at 37°C. Finally, bone sections were immunostained for BrdU as described in the Immunofluorescence Staining section.

Immunofluorescence Staining-Cells were fixed with 4% paraformaldehyde-PBS for 15min. Following permeabilization in PBS-TritonX100 (0.2%) and blocking with goat serum (PBS-Goat serum 10%), cells were incubated with primary antibodies during 1 hour. Secondary antibodies used were conjugated with Alexa 488 and Alexa 555 from Jackson Immunoresearch (Interchim, Montluçon, France). Samples were mounted using Mowiol 4-88 reagents (Sigma Aldrich, l'Isle d'Abeau, France) supplemented or not with DAPI (Life technologies, St Aubin, France) and were analyzed using Axioimager microscope or LSM 510 laser scanning confocal microscope (Carl Zeiss SAS, Le Pecq, France.).

Cell fractionation-All the operations were carried out at 4°C. Cells from 4 petri 10 cm dishes were washed twice with PBS then scrapped in 1mL PBS with a rubber policeman. They were centrifuged at 1500 rpm for 5 minutes. The pellet was re-suspended in a hypotonic buffer made of 10 mM HEPES pH 7.4, EDTA 1 mM, and a cocktail of protease inhibitors (Complete, Roche Diagnostic, Meylan, France) and phosphatase inhibitors (Sigma Aldrich, l'Isle d'Abeau, France), and incubated 10 min on ice. The cells were broken with a Dounce homogenizer (Piston B, 25 stokes). Unbroken cells and nucleus were eliminated by a centrifugation at 2500 rpm for 5 min. Mitochondria were further removed by a 6000-rpm centrifugation for 15 min.

For cytoplasm and total membrane recovery, the supernatant was centrifuged at 120000 rpm, 4°C, 20 min in a fixed angle AT120 rotor in a Hitachi micro ultracentrifuge. The whole membrane fraction was recovered from the pellet fraction after solubilizing in 50mM Tris pH7.4, 1% TritonX100, 150 mM NaCl, 1 mM EDTA, 20 min at 4°C. Cytoplasmic proteins were recovered from the previous supernatant.

RhoA and Rac activity- GST-Rhotekin and GST-PAK-Crib based pulldown assays were carried out as previously reported in (52).

Pharmacological inhibition of Rac and group I PAK- Cells were resuspended in DMEM and preincubated in suspension for 30min at 37°C. then either ETH1864 (53) or IPA3 (54) were added at the concentration of 50 µM and 10 µM, respectively, and the incubation pursued for another 30 min. The cells were then plated in the

presence of the inhibitors for one hour before fixation with PFA and Immunostaining.

Immunoprecipitations- GFP-Trap magnetic beads were used following manufacturer's instructions (Chromotek, Martinsried, Germany). Immunoprecipitation using the Flag epitope was done with M2 antibody coupled magnetic beads (Sigma Aldrich, L'Isle d'Abeau France).

Immunoblotting-Cells were lysed using RIPA lysis buffer containing proteases and phosphatases inhibitors. Cell lysates were centrifuged at 15 000rpm for 30 min at 4°C, and supernatants were used for immunoblotting using standard protocol.

RNA Extraction, Reverse Transcription, qPCR and transcriptomic analyses-Total RNA was isolated using TRIzol reagent (Thermo Fisher Scientific, Waltham, USA) and RNeasy Kit (Qiagen, Courtaboeuf, France) following the manufacturer's instructions. Total RNA quantification was performed using the Nanodrop ND- 1000 spectrophotometer (Thermo Fisher Scientific, Waltham, USA). RNA was reverse-transcribed with the iScript Reverse Transcription Supermix (Biorad, Hercules, USA). Real-time qPCR analysis was performed using iTaq Universal SybrGreen Supermix (Biorad, Hercules, USA) on Biorad CFX96. Primers list used for qPCR analysis is provided in Table EV7. The integrity of the extracted RNAs was assessed with the Bioanalyzer 2100 and the RNA6000 Nano kit (Agilent Technologies Incorporation, Santa Clara, USA). A RNA integrity number (RIN) greater or equal to 7.00 was achieved for all samples. No sign of DNA contamination was detected in any of the samples analyzed. The starting amount of total RNA used for the reactions was 400 nanograms per sample, for all samples. The Illumina Total Prep RNA Amplification Kit (Applied Biosystems / Ambion, Austin, USA) was used to generate biotinylated, amplified cRNA according to the manufacturer recommendations. Hybridization, staining and detection of cRNAs on Illumina Mouse WG-6 v2 Expression BeadChips were performed according to the manufacturer's protocol. The MouseWG-6 v2.0 BeadChip profiles more than 45,200 transcripts derived from the National Center for Biotechnology Information Reference Sequence (NCBI RefSeq) database (Build 36, Release 22), the Mouse Exonic Evidence Based Oligonucleotide (MEEBO) set as well as from exemplar protein-coding sequences described in the RIKEN FANTOM2 database. The Illumina I-Scan system was used to scan all Expression BeadChips, according to Illumina recommendations.

Using the Gene Expression Module 1.9.0 of GenomeStudio V2011.1 software (Illumina - USA), the Quantile normalization method was applied to the primary probe data. Processed probe data were then filtered according to the following criteria: minimal signal intensity fold change of 1.50 across all samples, minimal probe signal intensity absolute change of 150 across all samples. Filtered data were then log2-transformed, and the expression values compared between the $\beta1^{-/-}$ cells and wild-type $\beta1^{f/f}$ samples using Omics Explorer 3.2(42) (Qlucore, Sweden). Genes were considered differentially expressed when their expression level satisfied two criteria: the adjusted p-value (q-value) was < 0.01(which corresponded to a $|R| > 0.96$ ii) the absolute fold change between the mean expression value in the samples from mutant cells compared to that in controls was > 1.5. Two-dimension hierarchical clustering analysis was performed using Omics Explorer 3.2(42) software on normalized data (mean=0, variance=1) with the average linkage option.

Cell Proliferation Assay-Cells were treated with BrdU or alternatively with EdU (10µM, Sigma) during 1 hour or 30 min for osteoblasts and MEFs respectively. For BrdU staining, cells were fixed with Carnoy's fixative (75% methanol: 25% glacial acetic acid) 20 min at -20°C, and then denatured using 2M HCl 1hour at 37°C. Cells were then immunostained for BrdU as described earlier. BrdU positive cells were counted under Axioimager microscope (Carl Zeiss, Inc.). For EdU staining, manufacturer's protocol was used, after an incubation of cells with EdU for 30 minutes.

Quantification of YAP nuclear localization-Cells were immuno-stained with an anti YAP and immuno-microscopy was carried out with a confocal laser scanning microscope (Zeiss LSM510) equipped with a 63X planapo oil immersion objective (n.a. 1.4) and a pinhole set to one Airy. On each cell image a ROI was defined positioned either within the nuclei, or in the cytoplasmic area next to the nuclei envelope. Since the thickness of the two ROI positions were likely identical, the average fluorescence intensity is likely proportional to YAP concentration and was estimated using Image J public software. Within the same cell, the ratio of both fluorescence intensities reflects YAP concentration ratio in both compartments. This ratio was represented under a logarithmic scale in order to have an identical range for positive and negative ratios. Measurements were performed with $n \geq 50$ and statistical significance was estimated with Student test. Boxplots were performed using R public software.

Colocalization microscopy-Confocal images were taken using LSM510 Zeiss microscope. Visualization and quantification of colocalized pixels were carries out using Wright cell imaging (55) facility plugins of Image J. (http://wwwfacilities.uhnresearch.ca/wcif/imagej/colour_analysis.htm).

ACKNOLEDGMENTS

We are indebted to Pr. R. Fässler, Drs. A. McMahon, R. Meuwissen and T. Jacks for sharing their mice. We thank Dr Nachbrandi for histomorphometric analysis. We warmly thank Pr. J. Bos, Drs K.L. Guan, M. Barbacid, C. Gauthier-Rouvière, A. Mettouchi, and Dr Chernoff for their precious help in sharing their constructs. We also would like to thank Dr S. Dimitrov for his strong support. MB was supported with a fellowship from "Ministère de la Recherche" and INCa (Institut National du Cancer) grant.

CONFLICT OF INTEREST

The authors declare that they have no conflicts of interest with the contents of this article.

AUTHOR CONTRIBUTIONS

HS, MB, ASR, VM, GC, performed experiments. BW discuss the data and contributed to the redaction of the manuscript. PG designed and performed and analyzed transcriptomic data. MRB, DB, DL designed, performed experiments, analyzed data, and wrote the manuscript.

REFERENCES

1. Hynes, R. O. (1992) Integrins: versatility, modulation, and signaling in cell adhesion. *Cell* **69**, 11-25
2. Bouvard, D., Pouwels, J., De Franceschi, N., and Ivaska, J. (2013) Integrin inactivators: balancing cellular functions in vitro and in vivo. *Nat Rev Mol Cell Biol* **14**, 432-444
3. Assoian, R. K., and Schwartz, M. A. (2001) Coordinate signaling by integrins and receptor tyrosine kinases in the regulation of G1 phase cell-cycle progression. *Curr Opin Genet Dev* **11**, 48-53
4. Hirsch, E., Barberis, L., Brancaccio, M., Azzolino, O., Xu, D., Kyriakis, J. M., Silengo, L., Giancotti, F. G., Tarone, G., Fassler, R., and Altruda, F. (2002) Defective Rac-mediated proliferation and survival after targeted mutation of the beta1 integrin cytodomain. *J Cell Biol* **157**, 481-492
5. Zhao, B., Tumaneng, K., and Guan, K. L. (2011) The Hippo pathway in organ size control, tissue regeneration and stem cell self-renewal. *Nat Cell Biol* **13**, 877-883
6. Harvey, K. F., Pfleger, C. M., and Hariharan, I. K. (2003) The Drosophila Mst ortholog, hippo, restricts growth and cell proliferation and promotes apoptosis. *Cell* **114**, 457-467
7. Kanai, F., Marignani, P. A., Sarbassova, D., Yagi, R., Hall, R. A., Donowitz, M., Hisaminato, A., Fujiwara, T., Ito, Y., Cantley, L. C., and Yaffe, M. B. (2000) TAZ: a novel transcriptional co-activator regulated by interactions with 14-3-3 and PDZ domain proteins. *EMBO J* **19**, 6778-6791
8. Schlegelmilch, K., Mohseni, M., Kirak, O., Pruszak, J., Rodriguez, J. R., Zhou, D., Kreger, B. T., Vasioukhin, V., Avruch, J., Brummelkamp, T. R., and Camargo, F. D. (2011) Yap1 acts downstream of alpha-catenin to control epidermal proliferation. *Cell* **144**, 782-795
9. Meng, Z., Moroishi, T., and Guan, K. L. (2016) Mechanisms of Hippo pathway regulation. *Genes Dev* **30**, 1-17
10. Zhao, B., Li, L., Wang, L., Wang, C. Y., Yu, J., and Guan, K. L. (2012) Cell detachment activates the Hippo pathway via cytoskeleton reorganization to induce anoikis. *Genes Dev* **26**, 54-68
11. Kim, N.-G., and Gumbiner, B. M. (2015) Adhesion to fibronectin regulates Hippo signaling via the FAK-Src-PI3K pathway. *Journal of Cell Biology* **210**, 503–515
12. Huang, S., and Ingber, D. E. (2005) Cell tension, matrix mechanics, and cancer development. *Cancer Cell* **8**, 175-176
13. Howe, A. K., and Juliano, R. L. (2000) Regulation of anchorage-dependent signal transduction by protein kinase A and p21-activated kinase. *Nat Cell Biol* **2**, 593-600

14. Kim, M., Lee, S., Kuninaka, S., Saya, H., Lee, H., and Lim, D. S. (2013) cAMP/PKA signalling reinforces the LATS-YAP pathway to fully suppress YAP in response to actin cytoskeletal changes. *EMBO J* **32**, 1543-1555
15. Kim, N. G., and Gumbiner, B. M. (2015) Adhesion to fibronectin regulates Hippo signaling via the FAK-Src-PI3K pathway. *J Cell Biol* **210**, 503-515
16. Dupont, S., Morsut, L., Aragona, M., Enzo, E., Giulitti, S., Cordenonsi, M., Zanconato, F., Le Digabel, J., Forcato, M., Bicciato, S., Elvassore, N., and Piccolo, S. (2011) Role of YAP/TAZ in mechanotransduction. *Nature* **474**, 179-183
17. Sero, J. E., and Bakal, C. (2017) Multiparametric Analysis of Cell Shape Demonstrates that β-PIX Directly Couples YAP Activation to Extracellular Matrix Adhesion. *Cell Syst* **4**, 84-96.e86
18. Okada, T., Lopez-Lago, M., and Giancotti, F. G. (2005) Merlin/NF-2 mediates contact inhibition of growth by suppressing recruitment of Rac to the plasma membrane. *J Cell Biol* **171**, 361-371
19. Zhu, X., and Assoian, R. K. (1995) Integrin-dependent activation of MAP kinase: a link to shape-dependent cell proliferation. *Mol Biol Cell* **6**, 273-282
20. Ehmer, U., and Sage, J. (2016) Control of Proliferation and Cancer Growth by the Hippo Signaling Pathway. *Mol Cancer Res* **14**, 127-140
21. Elbediwy, A., Vincent-Mistiaen, Z. I., Spencer-Dene, B., Stone, R. K., Boeing, S., Wculek, S. K., Cordero, J., Tan, E. H., Ridgway, R., Brunton, V. G., Sahai, E., Gerhardt, H., Behrens, A., Malanchi, I., Sansom, O. J., and Thompson, B. J. (2016) Integrin signalling regulates YAP and TAZ to control skin homeostasis. *Development* **143**, 1674-1687
22. Johnson, L., Mercer, K., Greenbaum, D., Bronson, R. T., Crowley, D., Tuveson, D. A., and Jacks, T. (2001) Somatic activation of the K-ras oncogene causes early onset lung cancer in mice. *Nature* **410**, 1111-1116
23. Feng, X., Degese, M. S., Iglesias-Bartolome, R., Vaque, J. P., Molinolo, A. A., Rodrigues, M., Zaidi, M. R., Ksander, B. R., Merlino, G., Sodhi, A., Chen, Q., and Gutkind, J. S. (2014) Hippo-independent activation of YAP by the GNAQ uveal melanoma oncogene through a trio-regulated rho GTPase signaling circuitry. *Cancer Cell* **25**, 831-845
24. Reginensi, A., Scott, R. P., Gregorieff, A., Bagherie-Lachidan, M., Chung, C., Lim, D. S., Pawson, T., Wrana, J., and McNeill, H. (2013) Yap- and Cdc42-dependent nephrogenesis and morphogenesis during mouse kidney development. *PLoS Genet* **9**, e1003380
25. Das, S., Yin, T., Yang, Q., Zhang, J., Wu, Y. I., and Yu, J. (2015) Single-molecule tracking of small GTPase Rac1 uncovers spatial regulation of membrane translocation and mechanism for polarized signaling. *Proc Natl Acad Sci U S A* **112**, E267-276
26. Weed, S. A., Du, Y., and Parsons, J. T. (1998) Translocation of cortactin to the cell periphery is mediated by the small GTPase Rac1. *J Cell Sci* **111 (Pt 16)**, 2433-2443
27. Parrini, M. C., Camonis, J., Matsuda, M., and de Gunzburg, J. (2009) Dissecting activation of the PAK1 kinase at protrusions in living cells. *J Biol Chem* **284**, 24133-24143
28. Sells, M. A., Pfaff, A., and Chernoff, J. (2000) Temporal and spatial distribution of activated Pak1 in fibroblasts. *J Cell Biol* **151**, 1449-1458
29. Choma, D. P., Milano, V., Pumiglia, K. M., and DiPersio, C. M. (2007) Integrin alpha3beta1-dependent activation of FAK/Src regulates Rac1-mediated keratinocyte polarization on laminin-5. *J Invest Dermatol* **127**, 31-40
30. Feng, H., Hu, B., Liu, K. W., Li, Y., Lu, X., Cheng, T., Yiin, J. J., Lu, S., Keezer, S., Fenton, T., Furnari, F. B., Hamilton, R. L., Vuori, K., Sarkaria, J. N., Nagane, M., Nishikawa, R., Cavenee, W. K., and Cheng, S. Y. (2011) Activation of Rac1 by Src-dependent phosphorylation of Dock180(Y1811) mediates PDGFRα-stimulated glioma tumorigenesis in mice and humans. *J Clin Invest* **121**, 4670-4684

31. Yin, F., Yu, J., Zheng, Y., Chen, Q., Zhang, N., and Pan, D. (2013) Spatial organization of Hippo signaling at the plasma membrane mediated by the tumor suppressor Merlin/NF2. *Cell* **154**, 1342-1355
32. Shaw, R. J., Paez, J. G., Curto, M., Yaktine, A., Pruitt, W. M., Saotome, I., O'Bryan, J. P., Gupta, V., Ratner, N., Der, C. J., Jacks, T., and McClatchey, A. I. (2001) The Nf2 tumor suppressor, merlin, functions in Rac-dependent signaling. *Dev Cell* **1**, 63-72
33. Li, Y., Zhou, H., Li, F., Chan, S. W., Lin, Z., Wei, Z., Yang, Z., Guo, F., Lim, C. J., Xing, W., Shen, Y., Hong, W., Long, J., and Zhang, M. (2015) Angiomotin binding-induced activation of Merlin/NF2 in the Hippo pathway. *Cell Res* **25**, 801-817
34. Miyamoto, S., Teramoto, H., Gutkind, J. S., and Yamada, K. M. (1996) Integrins can collaborate with growth factors for phosphorylation of receptor tyrosine kinases and MAP kinase activation: roles of integrin aggregation and occupancy of receptors. *J Cell Biol* **135**, 1633-1642
35. Bouvier, C., Macagno, N., Nguyen, Q., Loundou, A., Jiguet-Jiglaire, C., Gentet, J. C., Jouve, J. L., Rochwerger, A., Mattei, J. C., Bouvard, D., and Salas, S. (2016) Prognostic value of the Hippo pathway transcriptional coactivators YAP/TAZ and β1-integrin in conventional osteosarcoma. *Oncotarget* **7**, 64702-64710
36. Faccio, R., Novack, D. V., Zallone, A., Ross, F. P., and Teitelbaum, S. L. (2003) Dynamic changes in the osteoclast cytoskeleton in response to growth factors and cell attachment are controlled by beta3 integrin. *J Cell Biol* **162**, 499-509
37. Matsumoto, S., Fujii, S., Sato, A., Ibuka, S., Kagawa, Y., Ishii, M., and Kikuchi, A. (2014) A combination of Wnt and growth factor signaling induces Arl4c expression to form epithelial tubular structures. *EMBO J* **33**, 702-718
38. Arthur, W. T., and Burridge, K. (2001) RhoA inactivation by p190RhoGAP regulates cell spreading and migration by promoting membrane protrusion and polarity. *Mol Biol Cell* **12**, 2711-2720
39. Gonzalez-Agosti, C., Xu, L., Pinney, D., Beauchamp, R., Hobbs, W., Gusella, J., and Ramesh, V. (1996) The merlin tumor suppressor localizes preferentially in membrane ruffles. *Oncogene* **13**, 1239-1247
40. Chang, F., Lemmon, C. A., Park, D., and Romer, L. H. (2007) FAK potentiates Rac1 activation and localization to matrix adhesion sites: a role for betaPIX. *Mol Biol Cell* **18**, 253-264
41. Dise, R. S., Frey, M. R., Whitehead, R. H., and Polk, D. B. (2008) Epidermal growth factor stimulates Rac activation through Src and phosphatidylinositol 3-kinase to promote colonic epithelial cell migration. *Am J Physiol Gastrointest Liver Physiol* **294**, G276-285
42. Palamidessi, A., Frittoli, E., Garré, M., Faretta, M., Mione, M., Testa, I., Diaspro, A., Lanzetti, L., Scita, G., and Di Fiore, P. P. (2008) Endocytic trafficking of Rac is required for the spatial restriction of signaling in cell migration. *Cell* **134**, 135-147
43. Robertson, L. K., and Ostergaard, H. L. (2011) Paxillin associates with the microtubule cytoskeleton and the immunological synapse of CTL through its leucine-aspartic acid domains and contributes to microtubule organizing center reorientation. *J Immunol* **187**, 5824-5833
44. Wickstrom, S. A., Lange, A., Hess, M. W., Polleux, J., Spatz, J. P., Kruger, M., Pfaller, K., Lambacher, A., Bloch, W., Mann, M., Huber, L. A., and Fassler, R. (2010) Integrin-linked kinase controls microtubule dynamics required for plasma membrane targeting of caveolae. *Dev Cell* **19**, 574-588
45. Potocnik, A. J., Brakebusch, C., and Fässler, R. (2000) Fetal and adult hematopoietic stem cells require beta1 integrin function for colonizing fetal liver, spleen, and bone marrow. *Immunity* **12**, 653-663
46. Rodda, S. J., and McMahon, A. P. (2006) Distinct roles for Hedgehog and canonical Wnt signaling in specification, differentiation and maintenance of osteoblast progenitors. *Development* **133**, 3231-3244

47. Tuveson, D. A., Shaw, A. T., Willis, N. A., Silver, D. P., Jackson, E. L., Chang, S., Mercer, K. L., Grochow, R., Hock, H., Crowley, D., Hingorani, S. R., Zaks, T., King, C., Jacobetz, M. A., Wang, L., Bronson, R. T., Orkin, S. H., DePinho, R. A., and Jacks, T. (2004) Endogenous oncogenic K-ras(G12D) stimulates proliferation and widespread neoplastic and developmental defects. *Cancer Cell* **5**, 375-387
48. Soleimani, M., and Nadri, S. (2009) A protocol for isolation and culture of mesenchymal stem cells from mouse bone marrow. *Nat Protoc* **4**, 102-106
49. Bouvard, D., Aszodi, A., Kostka, G., Block, M. R., Albiges-Rizo, C., and Faessler, R. (2007) Defective osteoblast function in ICAP-1-deficient mice. *Development* **134**, 2615-2625
50. Brunner, M., Millon-Fremillon, A., Chevalier, G., Nakchbandi, I. A., Mosher, D., Block, M. R., Albiges-Rizo, C., and Bouvard, D. (2011) Osteoblast mineralization requires beta1 integrin/ICAP-1-dependent fibronectin deposition. *J Cell Biol* **194**, 307-322
51. Bentmann, A., Kawelke, N., Moss, D., Zentgraf, H., Bala, Y., Berger, I., Gasser, J. A., and Nakchbandi, I. A. (2009) Circulating fibronectin affects bone matrix, whereas osteoblast fibronectin modulates osteoblast function. *J Bone Miner Res* **25**, 706-715
52. Dib, K., Melander, F., Axelsson, L., Dagher, M. C., Aspenström, P., and Andersson, T. (2003) Down-regulation of Rac activity during beta 2 integrin-mediated adhesion of human neutrophils. *J Biol Chem* **278**, 24181-24188
53. Shutes, A., Onesto, C., Picard, V., Leblond, B., Schweighoffer, F., and Der, C. J. (2007) Specificity and mechanism of action of EHT 1864, a novel small molecule inhibitor of Rac family small GTPases. *J Biol Chem* **282**, 35666-35678
54. Deacon, S. W., Beeser, A., Fukui, J. A., Rennefahrt, U. E., Myers, C., Chernoff, J., and Peterson, J. R. (2008) An isoform-selective, small-molecule inhibitor targets the autoregulatory mechanism of p21-activated kinase. *Chem Biol* **15**, 322-331
55. Ho, H. Y., Rohatgi, R., Lebensohn, A. M., Le, M., Li, J., Gygi, S. P., and Kirschner, M. W. (2004) Toca-1 mediates Cdc42-dependent actin nucleation by activating the N-WASP-WIP complex. *Cell* **118**, 203-216

FIGURE LEGENDS

Figure 1. β1 integrins regulate osteoblast cell proliferation *in vivo* and *in vitro.*

A. Histo-morphometric analysis of osteoblast number on wild-type ($\beta1^{f/f}$) and Osx-Cre; $\beta1^{f/f}$ ($\beta1^{Ost\text{-}KO}$) 30-days-old mice tibias. Graphs show the mean ± SD from five independent experiments

B. Quantification of apoptotic (TUNEL-positive) and proliferating (BrdU-positive) cells in periosteum and trabecular bone in wild-type and mutant 30-days-old mice tibias (p; periosteum; t; trabecular bone). n=50; statistical significance of differences assessed by a two-tailed unpaired Student's t-test, 3 independent experiments.

C. Representative TUNEL staining

D. BrdU staining on trabecular bone sections from wild-type and mutant mouse tibias (hc, hypertrophic cartilage; tb, trabecular bone; bm, bone marrow). Scale bar represent 40µm.

E. Images of BrdU staining of trabecular bone sections.

F. BrdU based quantification of the proliferation rate of β1f/f, β1-/- primary mouse embryonic fibroblasts. (statistical significance of differences assessed by a two-tailed unpaired Student's t-test, 3 independent experiments)

G. *In vitro* proliferation rate of wild-type ($\beta1^{f/f}$) and β1 integrin deficient ($\beta1^{-/-}$) osteoblasts. n=50; statistical significance of differences assessed by a two-tailed unpaired Student's t-test, 3 independent experiments.

H. BrdU based quantification of the proliferation rate of $\beta1^{f/f}$ and $\beta1^{-/-}$ osteoblasts, or $\beta1^{-/-}$ osteoblasts expressing human β1 integrin (rescue), constitutively active MEK (MEKQ56P), or nuclear active ERK fusion mutant (MEK/ERKLA). Statistical significance of differences assessed by a two-tailed unpaired Student's t-test, 3 independent experiments.

Figure 2. β1 integrins regulate YAP nuclear localization.

A. Immunostaining of YAP (red) and β1 integrins (9EG7, green) on $\beta1^{f/f}$; $\beta1^{-/-}$; and β1 rescued osteoblasts. Scale bar represents 10µm.

B. Statistical analysis of YAP nuclear to cytoplasm ratio, n>50 cells for each condition. $\beta1^{f/f}$ and $\beta1^{-/-}$ osteoblasts were spread overnight on fibronectin (10µg/ml). Represented in a logarithmic scale. n=50; statistical significance of differences assessed by a two-tailed unpaired Student's t-test, the box plot is representative of 3 independent experiments.

C. Immunolocalization of YAP in $\beta1^{f/f}$, $\beta1^{-/-}$ osteoblasts (independent second clone #4.6).

D. Immunolocalization of Flag-YAP (red) in $\beta1^{f/f}$, $\beta1^{-/-}$ osteoblasts using anti-flag antibody. Nuclei were stained with DAPI.

E. Immunolocalization of YAP (red) and phospho tyrosine (PY, 4G10) (green) in $\beta1^{+/-}$ K-$Ras^{G12D/+}$, $\beta1^{-/-}$; K-$Ras^{G12D/+}$ MEFs. Nuclei were stained with DAPI

F. Western blot analysis of YAP phosphorylation. YAP^{pS127} and total YAP in $\beta1^{f/f}$ and $\beta1^{-/-}$ osteoblasts after cell fractionation of the nuclear fraction (N) and cytoplasmic/membrane fraction (CM). Lamin B and tubulin were used as nuclear and cytoplasmic markers, respectively.

Figure 3. β1 integrins control proliferation via YAP transcriptional activity.

A. RT-qPCR analysis of gene expression in $\beta1^{-/-}$ osteoblasts normalized to $\beta1^{f/f}$ cells (green line, set to 1). Results form 4 independent experiments. Statistical significance of differences assessed by a two-tailed unpaired Student's t-test.

B. Analysis of YAP and LATS phosphorylation (YAP^{pS127}, $LATS1/2^{pS909}$), and total YAP and LATS in $\beta1^{f/f}$; $\beta1^{-/-}$; and β1 rescued osteoblasts. Actin is shown as loading control.

C. Immunostaining of YAP on $\beta1^{f/f}$ and $\beta1^{-/-}$ osteoblasts expressing or not the YAP5SA mutant. Scale bar represents 10µm.

D. RT-qPCR analysis of Cyr61 and CTGF mRNA in $\beta1^{f/f}$, $\beta1^{-/-}$ osteoblasts and $\beta1^{f/f}$, $\beta1^{-/-}$ osteoblasts expressing Flag-YAP5SA. Statistical significance of differences assessed by a two-tailed unpaired Student's t-test, 3 independent experiments.

E. BrdU based quantification of the proliferation rate of $\beta1^{f/f}$ and $\beta1^{-/-}$ osteoblasts expressing or not the YAP^{5SA} mutant. n=30; Statistical significance of differences assessed by a two-tailed unpaired Student's t-test, 3 independent experiments.

F. RT-qPCR analysis of CyclinD1 (CCND1), CyclinD2 (CCND2), p19Arf and p21CIP (CDKN1A) mRNAs in $\beta1^{-/-}$ and $\beta1^{f/f}$ osteoblasts expressing Flag-YAP^{5SA} normalized to $\beta1^{f/f}$ osteoblasts (set to 1,

green line). Statistical significance of differences assessed by a two-tailed unpaired Student's t-test, 3 independent experiments.

.

Figure 4. Rac1 and Cdc42 but not RhoA controls β1 dependent YAP nuclear translocation

A. Immunostaining of YAP (red) in $\beta1^{-/-}$ osteoblasts expressing or not GFP-$Rac1^{G12V}$., GFP-$Cdc42^{G12V}$, and GFP-$RhoA^{G14V}$. Scale bar represents 10µm.

B. Statistical analysis of YAP nuclear to cytoplasm ratio, n>50 cells, represented in a logarithmic scale. Control (Ctl) $\beta1^{f/f}$ and $\beta1^{-/-}$ cells, or $\beta1^{f/f}$ and $\beta1^{-/-}$ osteoblasts stably expressing $RhoA^{G14V}$ were spread on fibronectin (10µg/ml) and YAP subcellular localization was analyzed. Statistical significance of differences assessed by a two-tailed unpaired Student's t-test, The box plot is representative of 2 independent experiments.

C. GST-Rhotekin pulldown assay was performed on $\beta1^{f/f}$ and $\beta1^{-/-}$ cells. RhoA was analyzed by immunoblotting from the pulldown fraction (RhoA-GTP) and the input (total RhoA).

D. $\beta1^{f/f}$ and $\beta1^{-/-}$ cells were transiently transfected with pYFP-RhoA construct and 48h cells were fixed and analyzed by confocal microscopy.

E. Statistical analysis of YAP nuclear to cytoplasm ratio, n>50 cells, represented in a logarithmic scale. Control (Ctl) $\beta1^{f/f}$ and $\beta1^{-/-}$ cells or $\beta1^{-/-}$ osteoblasts stably expressing $Rac1^{G12V}$ or $Cdc42^{G12V}$ were spread on fibronectin (10µg/ml) and YAP subcellular localization was analyzed. Statistical significance of differences assessed by a two-tailed unpaired Student's t-test, the box plot is representative of 3 independent experiments.

F. Statistical analysis of cell spreading. The projected areas of $\beta1^{f/f}$, $\beta1^{-/-}$ $\beta1^{f/f}$ and $\beta1^{-/-}$ stably expressing Rac^{G12V} cells spread on fibronectin (10µg/ml) for 2 hours were estimated after labelling of the cell with Vybrant™ Dill and thresholding the image to fit the mask size to the cell geometry. Measurements were performed with Metamorph software. n>50 cells; statistical significance of differences assessed by a two-tailed unpaired Student's t-test. The boxplot is representative of 2 independent experiments.

Figure 5. Rac1 dependent activation of YAP and spatial distribution of Rac1 and its partners at cell membrane extensions.

A. Statistical analysis of YAP nuclear to cytoplasm ratio, represented in a logarithmic scale. Left panel: quantification of control (Ctl) $\beta1^{f/f}$ and $Cdc42^{N17}$ transfected cells. Right panel: quantification of (Ctl) $\beta1^{f/f}$ and ETH1864 treated cells (Rac inh). n>50 cells; statistical significance of differences assessed by a two-tailed unpaired Student's t-test; the box plot is representative of 2 independent experiments.

B. Cell proliferation quantification using EdU incorporation assay in control (Ctl) $\beta1^{f/f}$, $\beta1^{-/-}$ osteoblasts or $\beta1^{f/f}$ and $\beta1^{-/-}$ osteoblasts expressing $Rac1^{G12V}$ (Rac1*).

C. Western blot of total YAP and YAP^{pS127} in $\beta1^{f/f}$ and $\beta1^{-/-}$ osteoblasts expressing or not $Rac1^{G12V}$.

D. GST-CRIB-PAK pulldown assay was performed on $\beta1^{f/f}$ and $\beta1^{-/-}$ cells. Rac1 was analyzed by immunoblotting from the pulldown fraction (Rac1-GTP) and the input (total Rac1).

E. Immunostaining of endogenous Rac1 (green) in $\beta1^{f/f}$ or $\beta1^{-/-}$ osteoblasts Scale bar represents 10µm. Arrows indicate ruffles formation in which Rac1 accumulates.

F. Line profile analysis illustrating Rac1 distribution from the cell edge to the nucleus.

G. Localization of TagRFP-cortactin in $\beta1^{f/f}$ or $\beta1^{-/-}$ osteoblasts Scale bar represents 10µm.

H. Line profile analysis illustrating cortactin distribution from the cell edge to the cytosol.

Figure 6. The Rac substrate PAK1 acts downstream of β1 integrins to control adhesion dependent YAP localization

A. Western blot analysis of PAK1 and $PAK1^{pT423}$ in $\beta1^{f/f}$, $\beta1^{-/-}$ and $\beta1^{rescue}$ osteoblasts. Actin was used as loading control.

B. Western blot analysis of endogenous Rac1, GFP-Rac1 (GFP) and PAK1 in $\beta1^{f/f}$, $\beta1^{-/-}$and $\beta1^{-/-}$ stably expressing GFP-$Rac1^{G12V}$ after cell fractionation to isolate total cell membranes (M) and cytoplasm (C). Tubulin and RalA were used as cytoplasmic and membrane markers, respectively.

C. Right panel: Immunolocalization of YAP in $\beta1^{-/-}$ osteoblasts transiently transfected with the constitutively active eGFP-PAK1 ($PAK1^{T423E}$). Scale bar represents 10µm. Left panel: Statistical analysis of YAP nuclear to cytoplasm ratio in $\beta1^{-/-}$ and $\beta1^{-/-}$ transfected with activated PAK1. Cells were spread overnight on fibronectin (10µg/ml). n>20 cells, represented in a logarithmic scale. (statistical significance of differences assessed by a two-tailed unpaired Student's t-test, the box plot is representative of 2 independent experiments).

D. Statistical analysis of YAP nuclear to cytoplasm ratio, represented in a logarithmic scale. $\beta1^{f/f}$ were spread on fibronectin (10µg/ml) in the absence or presence of IPA3 (PAK Inh), then stained for YAP. n>50 cells; statistical significance of differences assessed by a two-tailed unpaired Student's t-test, the box plot is representative of 2 independent experiments.

E. Statistical analysis of YAP nuclear to cytoplasm ratio represented in a logarithmic scale. $\beta1^{f/f}$ were mock transfected (Ctl) or transfected with the dominant negative form of PAK1 ($PAK1^{K299R}$) and after 48 hours cells were seeded on fibronectin (10µg/ml) for 1 hour and processed for PAK1 and YAP immunostaining . PAK1 positive cells were selected to quantify YAP nuclear to cytoplasm ratio. n>30 cells; statistical significance of differences assessed by a two-tailed unpaired Student's t-test, the box plot is representative of 2 independent experiments.

Figure 7. Src regulates YAP nuclear translocation upstream of Rac1 and downstream of β1 integrins.

A. Western blot analysis of Src activation upon serum stimulation. $\beta1^{f/f}$ and $\beta1^{-/-}$ osteoblasts were serum starved overnight and then serum (10%) was added to the cells. Phosphorylation of Src and YAP as well as total amount were analyzed by Western blotting. Actin was used as loading control.

B. EdU based quantification of the proliferation rate of $\beta1^{f/f}$ and $\beta1^{-/-}$ osteoblasts expressing or not (Ctl) the constitutively active form of Src (Src^{YF}). n=50; statistical significance of differences assessed by a two-tailed unpaired Student's t-test, 2 independent experiments.

C. Immunostaining of YAP (red) in $\beta1^{f/f}$ and $\beta1^{-/-}$ osteoblasts stably expressing or not the constitutively active form of Src (Src^{YF}). Most right panel: $\beta1^{-/-}$ osteoblasts expressing Src^{YF} were treated with ETH1864 for 3 hours prior to YAP staining. Scale bar represents 10µm.

D. Statistical analysis of YAP nuclear to cytoplasm ratio, represented in a logarithmic scale. $\beta1^{f/f}$, $\beta1^{-/-}$, $\beta1^{-/-}$ expressing a constitutively active form of Src (Src^{YF}) without (Ctl) or with ETH1864 (Rac inh) treatment. n>50 cells; statistical significance of differences assessed by a two-tailed unpaired Student's t-test, the box plot is representative of 2 independent experiments.

E. Western blot analysis of PAK1 activation. $\beta1^{f/f}$ and $\beta1^{-/-}$ osteoblasts expressing or not the constitutively active form of Src (Src^{YF}) were analyzed for phosphorylated PAK1 (p423, activated form) and total PAK1. Actin was used as loading control

Figure 8. β1 integrins control of YAP nuclear translocation in a merlin dependent manner.

A. Western blot analysis of NF2 and NF2 ^{pS518} in β1 deficient and $\beta1^{f/f}$ osteoblasts.

B. Western bot analysis of GFP trap performed with whole length, N-terminal FERM domain and C-terminal domain, as well as the S518 mutant of merlin to analyze interaction with LATS. Note that the S518 mutation decrease LATS interaction

C. Immunostaining of YAP (red) in $\beta1^{f/f}$ and $\beta1^{-/-}$ osteoblasts (Ctl), or stably expressing $NF2^{BB}$ mutant. Scale bar represents 10µm.

D. Statistical analysis of YAP nuclear to cytoplasm ratio, n>50 cells, represented in a logarithmic scale. $\beta1^{f/f}$, $\beta1^{-/-}$, $\beta1^{f/f}$ expressing $NF2^{BB}$ and $\beta1^{-/-}$ expressing $NF2^{BB}$ osteoblasts were spread on fibronectin (10µg/ml) and then stained for YAP. Statistical significance of differences assessed by a two-tailed unpaired Student's t-test, the box plot is representative of 2 independent experiments)

E. Western blot analysis of YAP, YAP^{pS127}, and merlin/NF2 (NF2) in $\beta1^{f/f}$, $\beta1^{-/-}$ expressing or not the $NF2^{BB}$ mutant. Actin was used as loading control.

F. EdU based quantification of the proliferation rate of $\beta1^{f/f}$ and $\beta1^{-/-}$ osteoblasts expressing or not (Ctl) the $NF2^{BB}$ mutant. n=50; statistical significance of differences assessed by a two-tailed unpaired Student's t-test, 2 independent experiments.

G. RT-qPCR analysis of gene expression in $\beta1^{-/-}$ and β1-/- expressing $NF2^{BB}$ osteoblasts gene expression was normalized to $\beta1^{f/f}$ cells (green line, set to 1). Mean SD value of 4 independent experiments.

H. Left panel: Statistical analysis of YAP nuclear to cytoplasm ratio, represented in a logarithmic scale. $\beta1^{f/f}$ and $\beta1^{f/f}$ expressing $NF2^{BB}$ were spread on fibronectin (10µg/ml) in the absence or presence of the Rac inhibitor ETH1864, then stained for YAP. n>50 cells; statistical significance of differences assessed by a two-tailed unpaired Student's t-test, the box plot is representative of 2 independent experiments. Right panel: Statistical analysis of YAP nuclear to cytoplasm ratio, represented in a logarithmic scale. $\beta1^{f/f}$ and $\beta1^{f/f}$ osteoblasts expressing $NF2^{BB}$ were spread on fibronectin (10µg/ml) in the absence or presence of IPA3, then stained for YAP. n>50 cells; statistical significance of differences assessed by a two-tailed unpaired Student's t-test, the box plot is representative of 2 independent experiments.

Figure -9. Cellular localization of YAP and interactors at the cell edges.

A. Immunostaining of YAP (red) and LATS (green, upper panel) or NF2/merlin (green, lower panel) on $\beta1^{f/f}$ osteoblasts. Scale bar represents 10µm. Quantitative analysis by intensity correlation was performed to visualize and quantify the colocalization.

B. Immunostaining of YAP (red) and YAP^{pS127} (green) on $\beta1^{f/f}$ osteoblasts (upper panels) or $\beta1^{-/-}$ (lower panels). Scale bar represents 10µm. Quantitative analysis by intensity correlation was performed to visualize and quantify the colocalization between YAP and its phosphorylated form.
C. Immunostaining of YAP (green) and Rac1 (red) on $\beta1^{f/f}$ osteoblasts (upper panels) or $\beta1^{-/-}$ (lower panels). Scale bar represents 10µm.
D. Immunolocalization of YAP (green) and TagRFP-cortactin in membrane extensions in $\beta1^{f/f}$ osteoblasts spread on fibronectin (10 µg/ml). Scale bar represents 10 µm.

Figure 10. Mapping interactions in merlin/NF2 complex.
A. Mapping of YAP binding site on merlin. Note that the S518 mutation decrease YAP interaction although the residue does not belong to the mapped binding site.
B. Western blot analysis of merlin/NF2 (NF2) and YAP from $\beta1^{f/f}$ and $\beta1^{-/-}$ stably expressing Flag-YAP. Cells were fractionated to isolate total cell membranes from the cytoplasm; then YAP was immunoprecipitated using the flag epitope. The presence of merlin was visualized in the different fractions. Merlin was also immunoblotted from the input fraction.
C. Western blot analysis of merlin/NF2 (NF2) and YAP from $\beta1^{f/f}$ and IPA3 treated cells stably expressing Flag-YAP. Cells were fractionated to isolate the total cell membranes and the cytoplasm; then YAP was immunoprecipitated using the flag epitope. The presence of merlin was visualized in different fractions. Merlin was also immunoblotted from the input fraction.
D. Summary of the β1 integrin control on YAP/merlin activation.

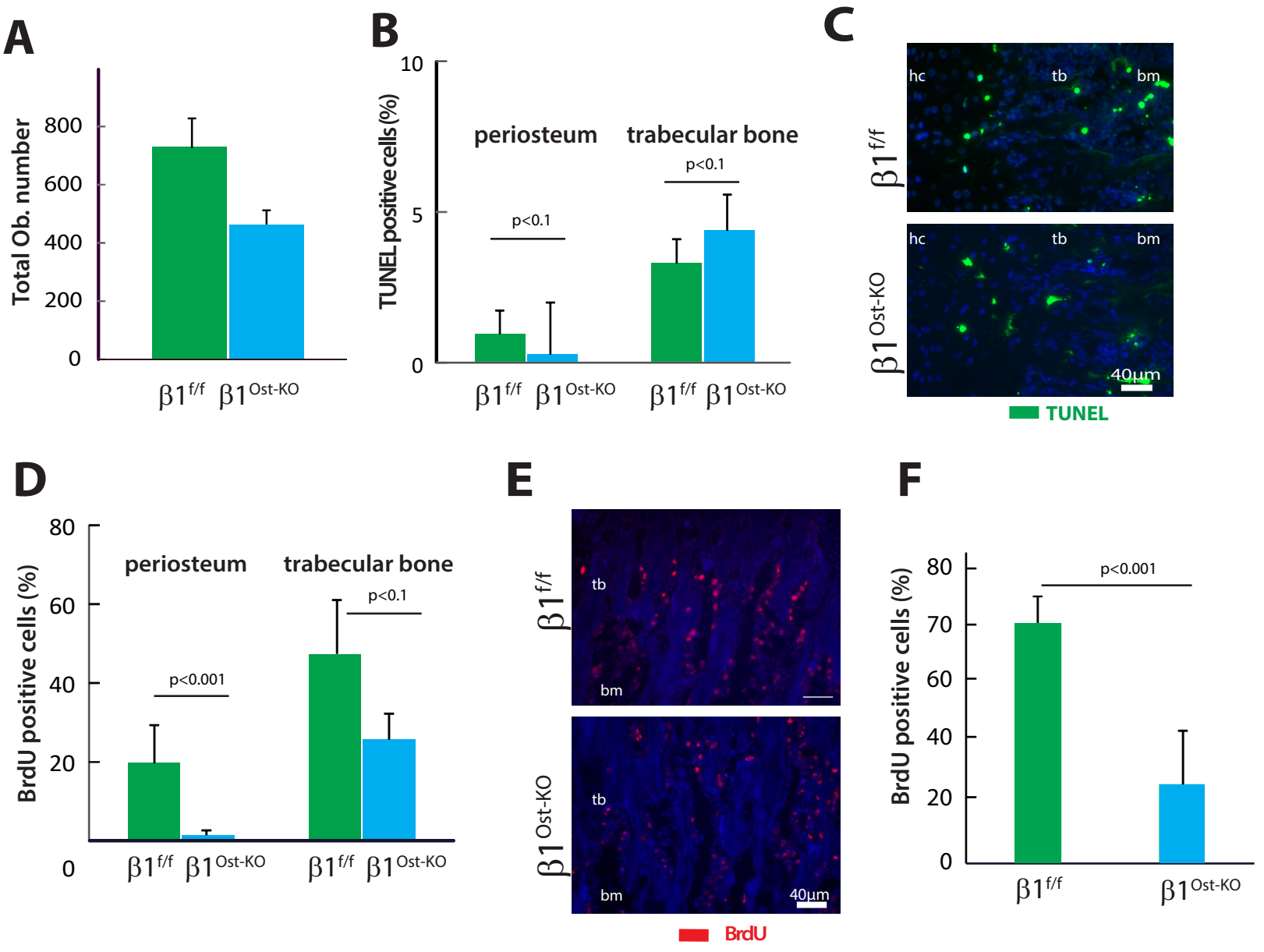
A
Total Ob. number
800
600
400
200
0
β1f/f
β1Ost-KO
B
TUNEL positive cells (%)
10
5
0
periosteum
trabecular bone
p<0.1
p<0.1
β1f/f
β1Ost-KO
β1f/f
β1Ost-KO
C
hc
tb
bm
β1f/f
hc
tb
bm
β1Ost-KO
40μm
TUNEL
D
BrdU positive cells (%)
80
60
40
20
0
periosteum
trabecular bone
p<0.001
p<0.1
β1f/f
β1Ost-KO
β1f/f
β1Ost-KO
E
β1f/f
tb
bm
β1Ost-KO
tb
bm
40μm
BrdU
F
BrdU positive cells (%)
80
70
60
40
20
0
p<0.001
β1f/f
β1Ost-KO
G
BrdU positive cells (%)
100
80
60
40
20
0
p<0.001
β1f/f
β1-/-
H
BrdU positive cells (%)
80
60
40
20
0
p<0.001
p<0.001
p<0.001
p<1
p<0.1
p<0.1
β1f/f
β1resc
β1-/-
MEKQ56P
MEK/ERK LA
β1-/-

Figure 1

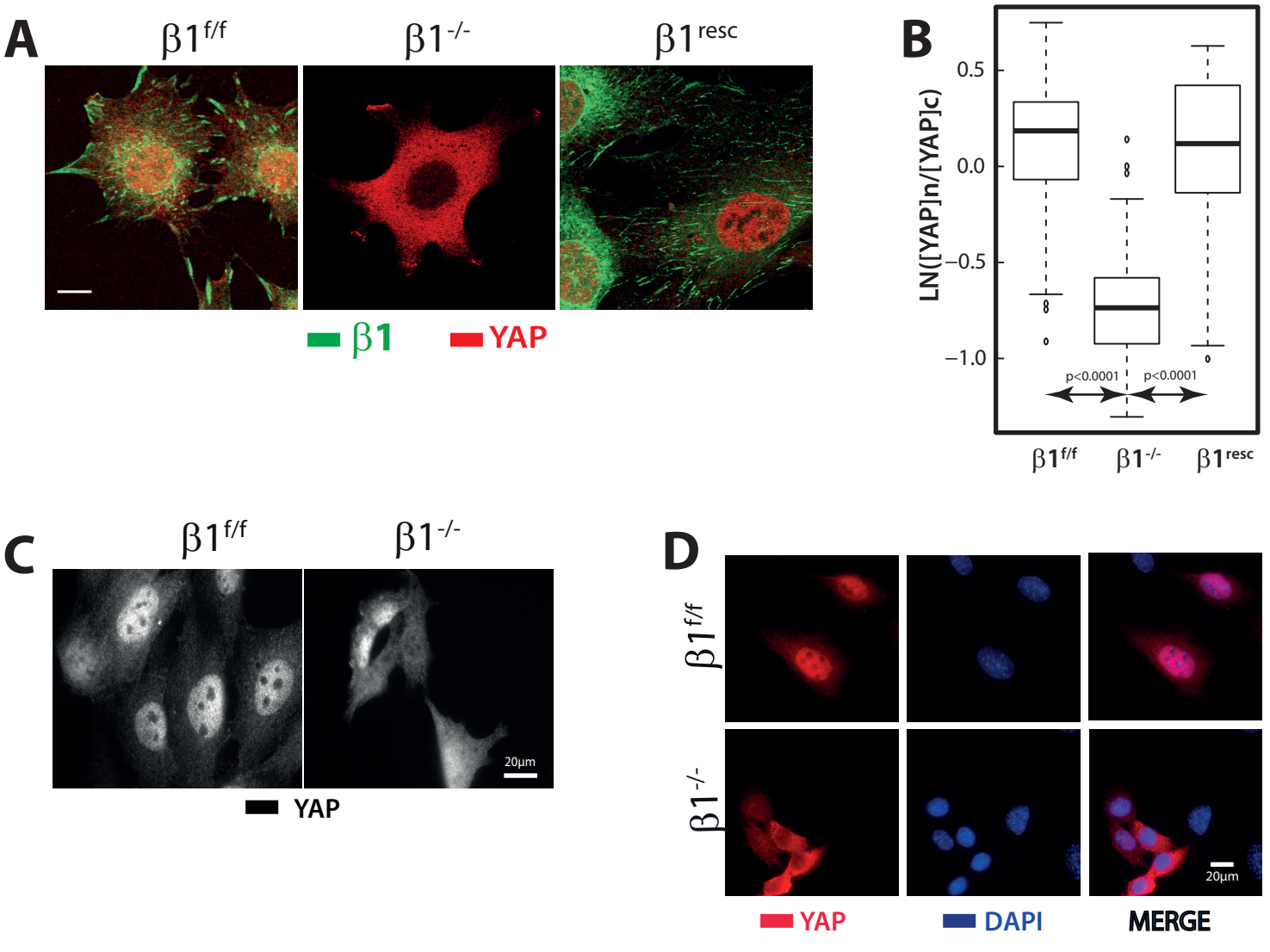
A
β1f/f
β1-/-
β1resc
β1
YAP
B
LN([YAP]n/[YAP]c)
0.5
0.0
−0.5
−1.0
p<0.0001
p<0.0001
β1f/f
β1-/-
β1resc
C
β1f/f
β1-/-
20μm
YAP
D
β1f/f
β1-/-
20μm
YAP
DAPI
MERGE
E
K-Ras G12D
β1-/f
β1-/-
20μm
YAP
PY
MERGE
F
β1f/f
β1-/-
N
CM
N
CM
YAP
YAPpS127
Lamin B
Tubulin
70 KD
70 KD
70 KD
55 KD

Figure 2

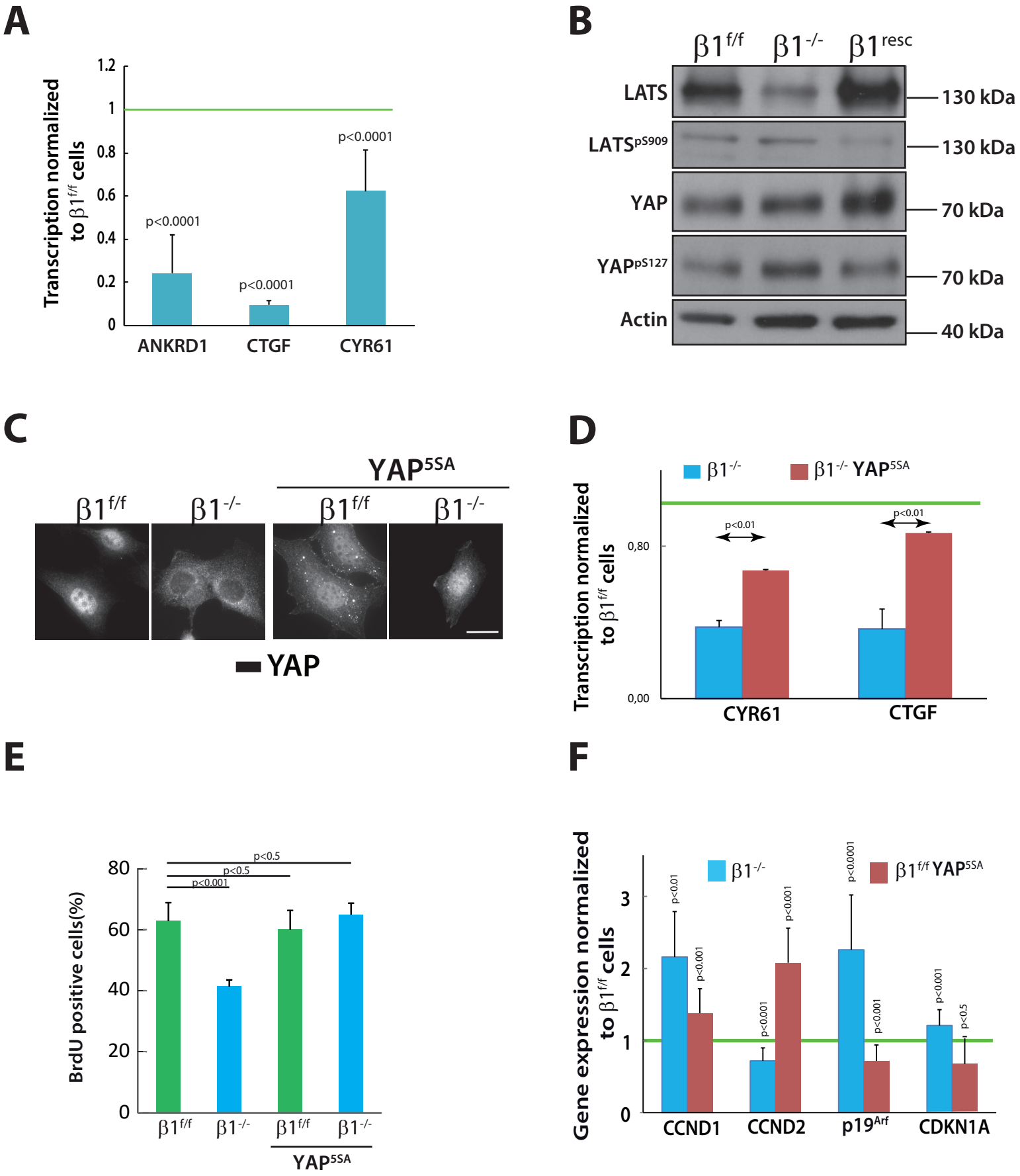
A
Transcription normalized to β1f/f cells
1.2
1
0.8
0.6
0.4
0.2
0
p<0.0001
p<0.0001
p<0.0001
ANKRD1
CTGF
CYR61
B
β1f/f
β1-/-
β1resc
LATS
LATSpS909
YAP
YAPpS127
Actin
130 kDa
130 kDa
70 kDa
70 kDa
40 kDa
C
YAP5SA
β1f/f
β1-/-
β1f/f
β1-/-
YAP
D
β1-/-
β1-/- YAP5SA
Transcription normalized to β1f/f cells
0,80
0,00
p<0.01
p<0.01
CYR61
CTGF
E
BrdU positive cells(%)
80
60
40
20
0
p<0.5
p<0.5
p<0.001
β1f/f
β1-/-
β1f/f
β1-/-
YAP5SA
F
β1-/-
β1f/f YAP5SA
Gene expression normalized to β1f/f cells
3
2
1
0
p<0.01
p<0.001
p<0.001
p<0.001
p<0.0001
p<0.001
p<0.001
p<0.5
CCND1
CCND2
p19Arf
CDKN1A

Figure 3

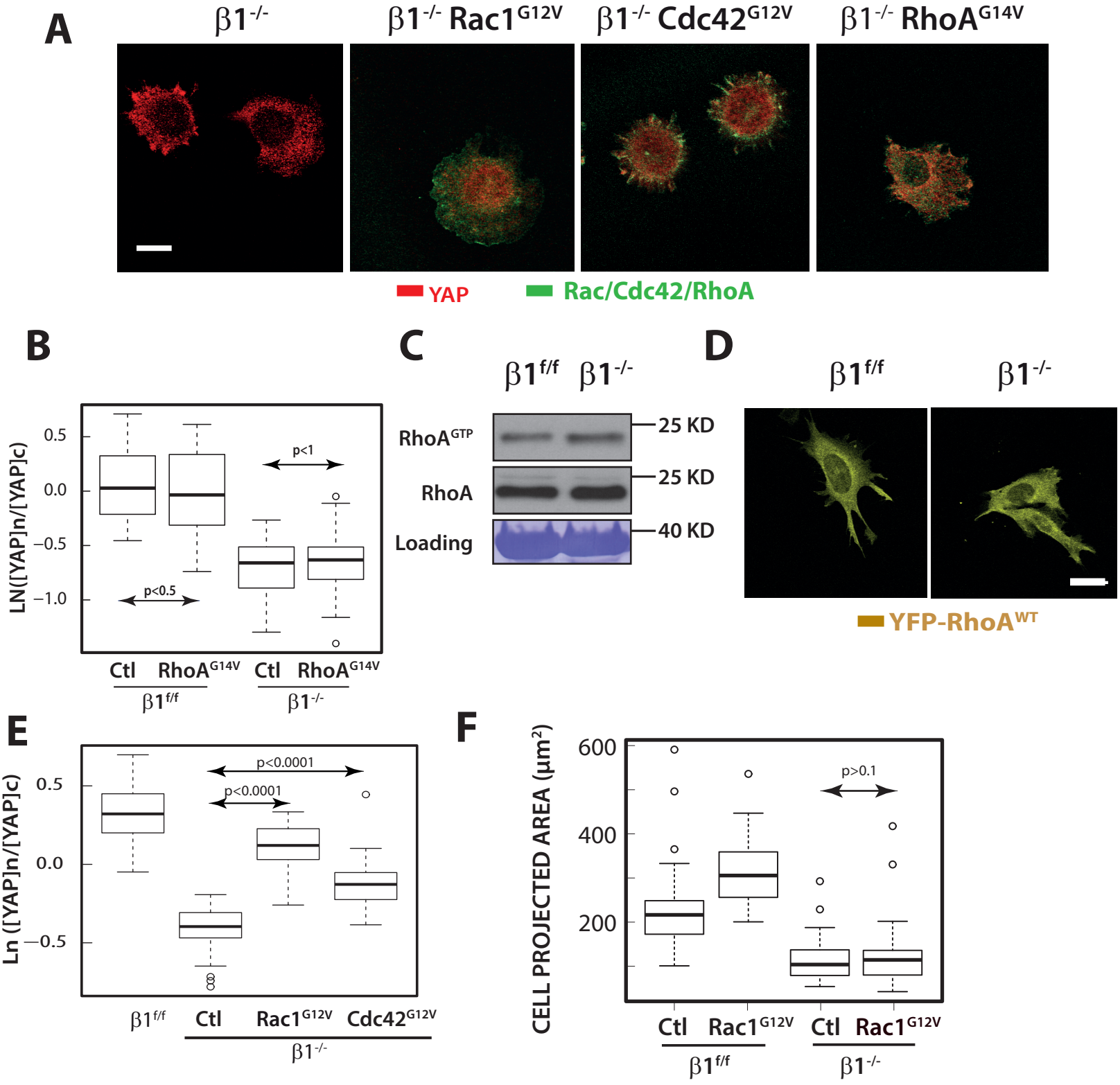
A
β1-/-
β1-/- Rac1G12V
β1-/- Cdc42G12V
β1-/- RhoAG14V
YAP
Rac/Cdc42/RhoA
B
LN([YAP]n/[YAP]c)
0.5
0.0
−0.5
−1.0
p<1
p<0.5
Ctl
RhoAG14V
Ctl
RhoAG14V
β1f/f
β1-/-
C
β1f/f
β1-/-
RhoAGTP
RhoA
Loading
25 KD
25 KD
40 KD
D
β1f/f
β1-/-
YFP-RhoAWT
E
Ln ([YAP]n/[YAP]c)
0.5
0.0
−0.5
p<0.0001
p<0.0001
β1f/f
Ctl
Rac1G12V
Cdc42G12V
β1-/-
F
CELL PROJECTED AREA (μm²)
600
400
200
p>0.1
Ctl
Rac1G12V
Ctl
Rac1G12V
β1f/f
β1-/-

Figure 4

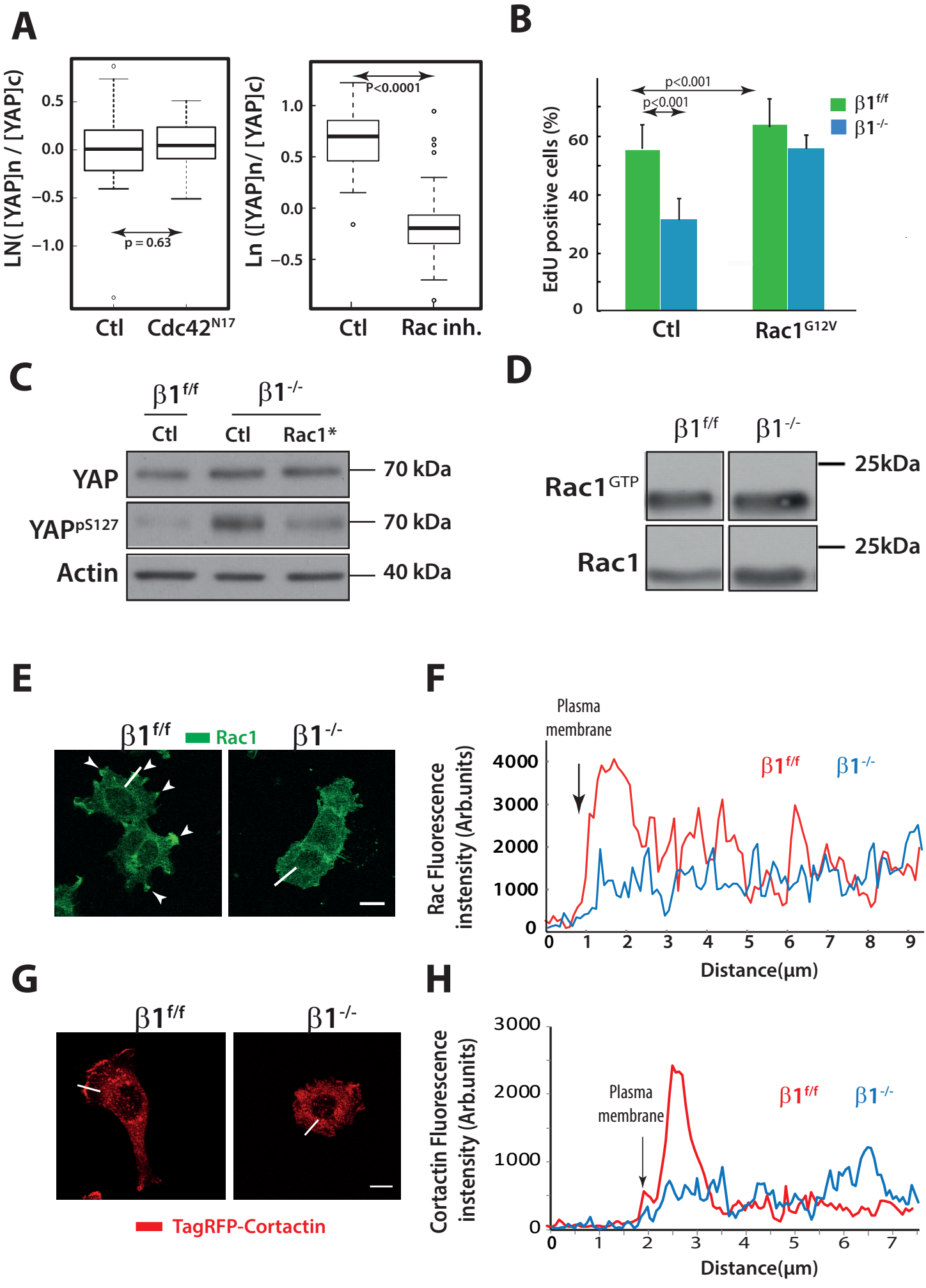
A
LN([YAP]n / [YAP]c)
0.5
0.0
−0.5
−1.0
p = 0.63
Ctl
Cdc42N17
Ln ([YAP]n/ [YAP]c)
P<0.0001
1.0
0.5
0.0
−0.5
Ctl
Rac inh.
B
EdU positive cells (%)
p<0.001
p<0.001
β1f/f
β1-/-
60
40
20
0
Ctl
Rac1G12V
C
β1f/f
β1-/-
Ctl
Ctl
Rac1*
YAP
YAPpS127
Actin
70 kDa
70 kDa
40 kDa
D
β1f/f
β1-/-
Rac1GTP
Rac1
25kDa
25kDa
E
β1f/f
Rac1
β1-/-
F
Plasma membrane
β1f/f
β1-/-
Rac Fluorescence instensity (Arb.units)
4000
3000
2000
1000
0
0 1 2 3 4 5 6 7 8 9
Distance(μm)
G
β1f/f
β1-/-
TagRFP-Cortactin
H
Cortactin Fluorescence instensity (Arb.units)
3000
2000
1000
0
Plasma membrane
β1f/f
β1-/-
0 1 2 3 4 5 6 7
Distance(μm)

Figure 5

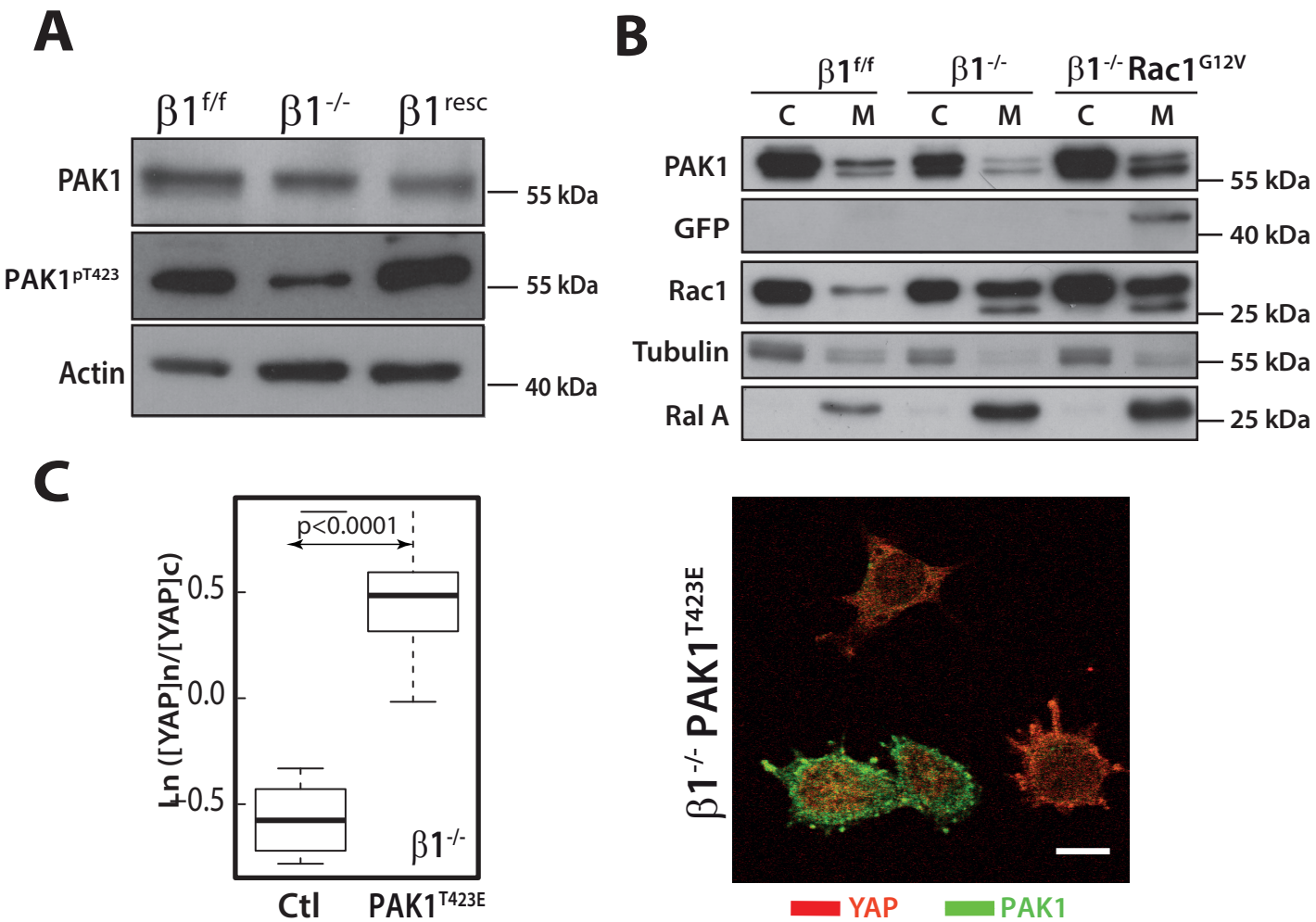
A
β1f/f
β1-/-
β1resc
PAK1
PAK1pT423
Actin
55 kDa
55 kDa
40 kDa
B
β1f/f
β1-/-
β1-/- Rac1G12V
C
M
C
M
C
M
PAK1
GFP
Rac1
Tubulin
Ral A
55 kDa
40 kDa
25 kDa
55 kDa
25 kDa
C
p<0.0001
Ln ([YAP]n/[YAP]c)
0.5
0.0
−0.5
β1-/-
Ctl
PAK1T423E
β1-/- PAK1T423E
YAP
PAK1
D
p<0.0001
Ln ([YAP]n/[YAP]c)
1.0
0.5
0.0
−0.5
−1.0
Ctl
PAK inh
E
p<0.0001
Ln ([YAP]n/[YAP]c)
1.0
0.5
0.0
−0.5
Ctl
PAK1K299R

Figure 6

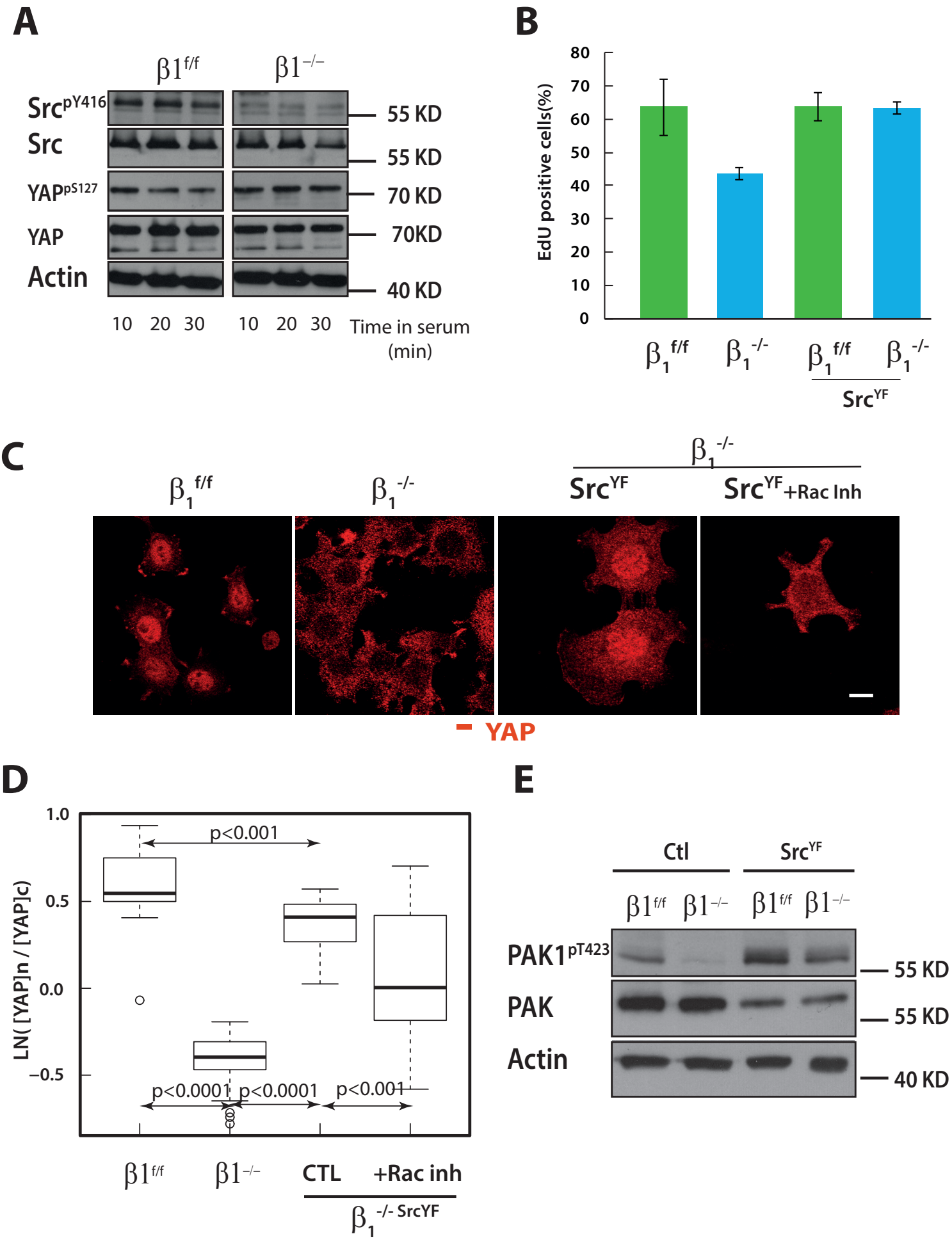
A
β1f/f
β1−/−
SrcpY416
Src
YAPpS127
YAP
Actin
55 KD
55 KD
70 KD
70KD
40 KD
10 20 30 10 20 30
Time in serum (min)
B
EdU positive cells(%)
80
70
60
50
40
30
20
10
0
β1 f/f
β1 -/-
β1 f/f
β1 -/-
SrcYF
C
β1 -/-
β1 f/f
β1 -/-
SrcYF
SrcYF+Rac Inh
YAP
D
1.0
0.5
0.0
−0.5
LN([YAP]n / [YAP]c)
p<0.001
p<0.0001
p<0.0001
p<0.001
β1f/f
β1−/−
CTL
+Rac inh
β1 -/- SrcYF
E
Ctl
SrcYF
β1f/f
β1−/−
β1f/f
β1−/−
PAK1pT423
PAK
Actin
55 KD
55 KD
40 KD

Figure 7

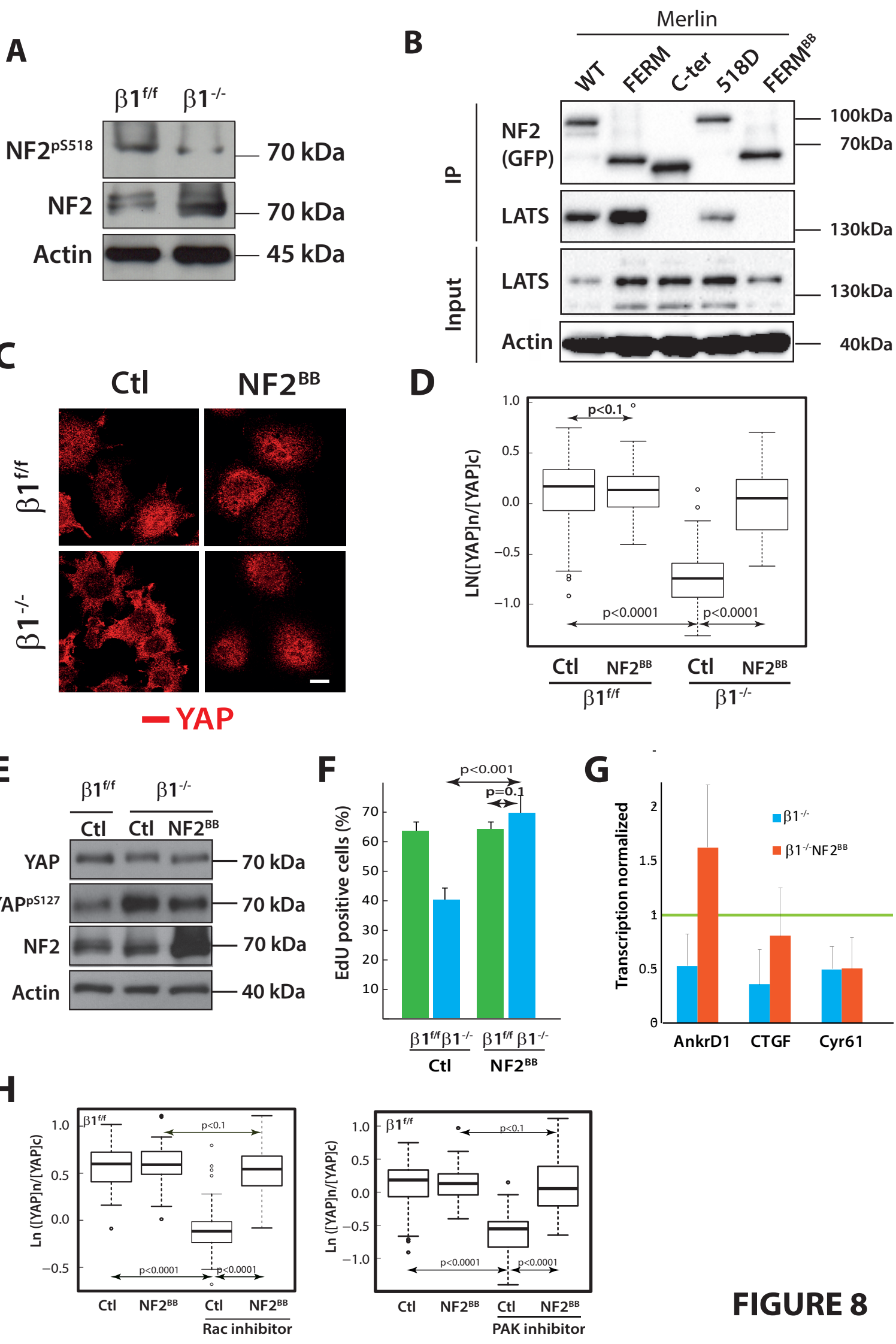
A
β1f/f
β1-/-
NF2pS518
NF2
Actin
70 kDa
70 kDa
45 kDa
B
Merlin
WT
FERM
C-ter
518D
FERMBB
IP
NF2 (GFP)
LATS
Input
LATS
Actin
100kDa
70kDa
130kDa
130kDa
40kDa
C
Ctl
NF2BB
β1f/f
β1-/-
YAP
D
LN([YAP]n/[YAP]c)
p<0.1
p<0.0001
p<0.0001
Ctl
NF2BB
Ctl
NF2BB
β1f/f
β1-/-
E
β1f/f
β1-/-
Ctl
Ctl
NF2BB
YAP
YAPpS127
NF2
Actin
70 kDa
70 kDa
70 kDa
40 kDa
F
EdU positive cells (%)
p<0.001
p=0.1
β1f/fβ1-/-
β1f/f β1-/-
Ctl
NF2BB
G
Transcription normalized
β1-/-
β1-/-NF2BB
AnkrD1
CTGF
Cyr61
H
β1f/f
Ln ([YAP]n/[YAP]c)
p<0.1
p<0.0001
p<0.0001
Ctl
NF2BB
Ctl
NF2BB
Rac inhibitor
β1f/f
Ln ([YAP]n/[YAP]c)
p<0.1
p<0.0001
p<0.0001
Ctl
NF2BB
Ctl
NF2BB
PAK inhibitor

FIGURE 8

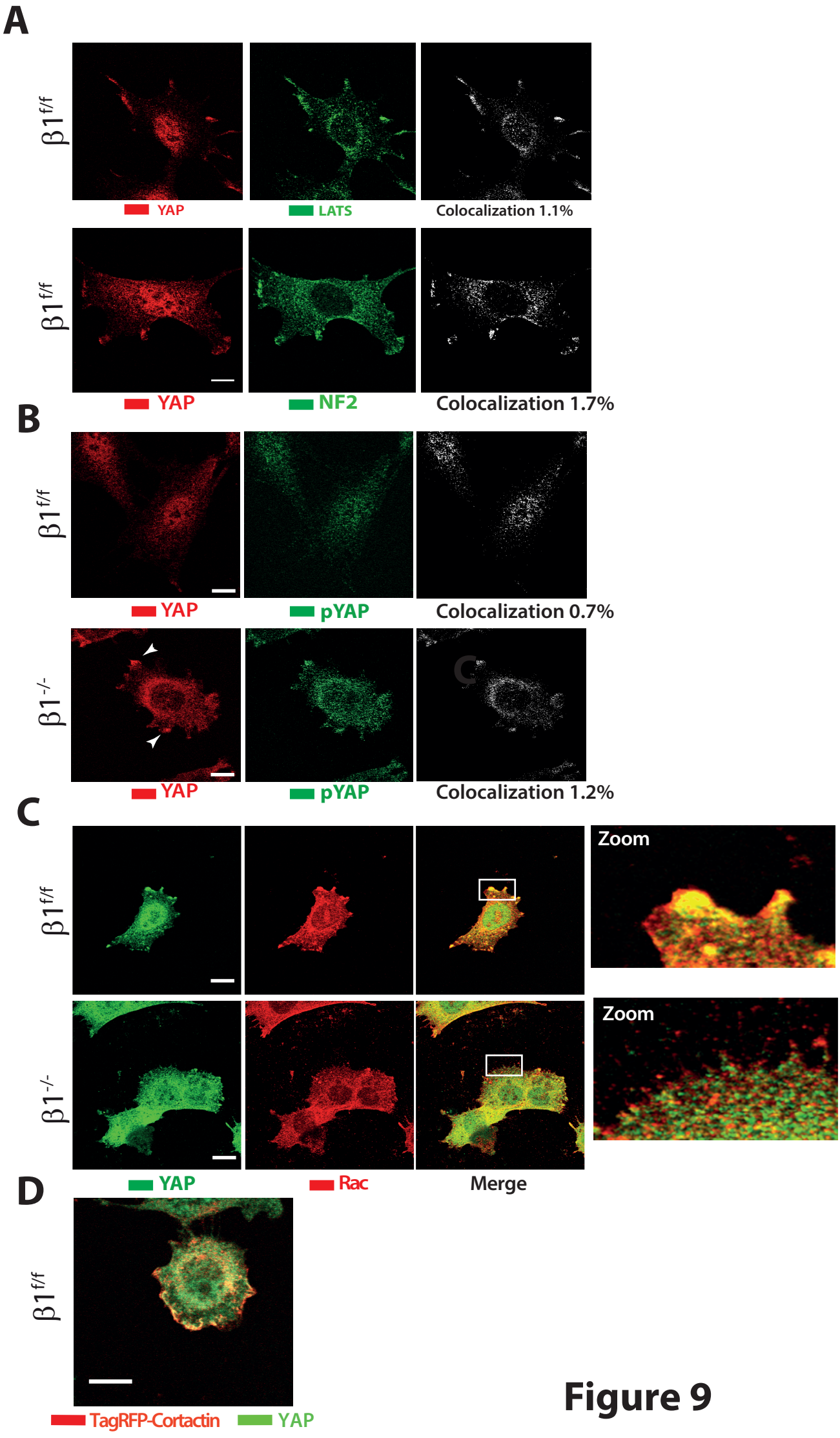
A
β1 f/f
YAP
LATS
Colocalization 1.1%
β1 f/f
YAP
NF2
Colocalization 1.7%
B
β1 f/f
YAP
pYAP
Colocalization 0.7%
β1 -/-
YAP
pYAP
Colocalization 1.2%
C
β1 f/f
Zoom
β1 -/-
Zoom
YAP
Rac
Merge
D
β1 f/f
TagRFP-Cortactin
YAP

Figure 9

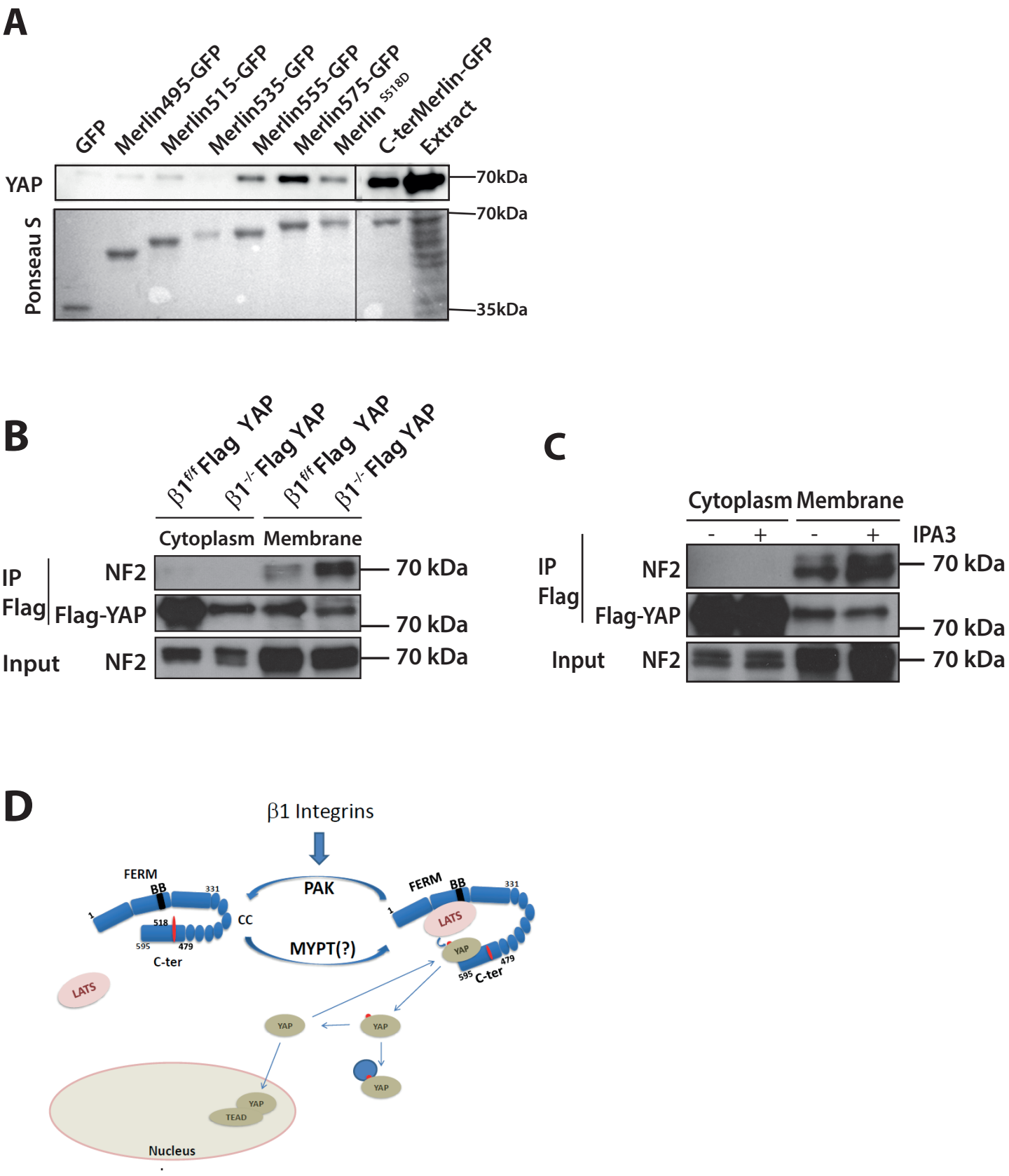
A
GFP
Merlin495-GFP
Merlin515-GFP
Merlin535-GFP
Merlin555-GFP
Merlin575-GFP
Merlin S518D
C-terMerlin-GFP
Extract
YAP
70kDa
Ponseau S
70kDa
35kDa
B
β1f/f Flag YAP
β1-/- Flag YAP
β1f/f Flag YAP
β1-/- Flag YAP
Cytoplasm
Membrane
IP Flag
NF2
Flag-YAP
Input
NF2
70 kDa
70 kDa
70 kDa
C
Cytoplasm
Membrane
- + - +
IPA3
IP Flag
NF2
Flag-YAP
Input
NF2
70 kDa
70 kDa
70 kDa
D
β1 Integrins
PAK
MYPT(?)
FERM
BB
331
1
518
595
479
C-ter
CC
LATS
YAP
TEAD
Nucleus

Figure 10